

THESIS FOR THE DEGREE OF DOCTOR OF PHILOSOPHY IN THERMO AND  
FLUID DYNAMICS

# Particulate Formation in GDI Engines

Towards sustainable transportation with zero emissions

SREELEKHA ETIKYALA



Department of Mechanics and Maritime Sciences  
*Division of Combustion and Propulsion Systems*  
CHALMERS UNIVERSITY OF TECHNOLOGY

Gothenburg, Sweden 2022

Particulate Formation in GDI Engines  
Towards sustainable transportation with zero emissions  
SREELEKHA ETIKYALA  
ISBN 978-91-7905-745-9

© SREELEKHA ETIKYALA, 2022

Department of Mechanics and Maritime Sciences  
Division of Combustion and Propulsion Systems  
Chalmers University of Technology  
SE-412 96 Gothenburg  
Sweden  
Telephone: +46 (0)31-772 1419

Cover:  
Illustration of particulate formation in a GDI engine by the author

Chalmers Reproservice  
Gothenburg, Sweden 2022

# ABSTRACT

The need to comply with stringent emission regulations while improving fuel economy and reducing criteria pollutant emissions from transportation presents a major challenge in the design of gasoline Direct Injection (DI) engines because of the adverse effects of ultrafine Particulate Number (PN) emissions on human health and other environmental concerns. With upcoming advances in vehicle electrification, it may be the case that electric vehicles completely replace all current vehicles powered by internal combustion engines ensuring zero emissions. In the meantime, Gasoline Direct Injection (GDI) engines have become the primary mode of transportation using gasoline as they offer better fuel economy while also providing low CO<sub>2</sub> emissions. However, GDI engines tend to produce relatively high PN emissions when compared to conventional Port Fuel Injection (PFI) engines, largely because of challenges associated with in-cylinder liquid fuel injection. Cold-starts, transients, and high load operation generate a disproportionate share of PN emissions from GDI engines over a certification cycle. The mechanisms of PN formation during these stages must therefore be understood to identify solutions that reduce overall PN emissions in order to comply with increasingly strict emissions standards.

This work presents experimental studies on particulate emissions from a naturally aspirated single cylinder metal gasoline engine run in a homogeneous configuration. The engine was adapted to enable operation in both DI and PFI modes. In PFI mode, injection was performed through a custom inlet manifold about 50 cm from the cylinder head to maximize the homogeneity of the fuel-air mixture. The metal head was eventually modified by incorporating an endoscope that made it possible to visualize the combustion process inside the cylinder. The experimental campaigns were structured to systematically isolate and clarify PN formation mechanisms. Tests were initially performed in steady state mode to obtain preliminary insights and to screen operating conditions before conducting transient tests. Particulate emissions were measured and correlated with the images obtained through endoscope visualization where possible.

Key objectives of these studies were to find ways of reducing PN formation by increasing combustion stability. It was found that by avoiding conditions that cause wall wetting with liquid fuel, PN emissions can be substantially reduced during both steady state operation and transients. Warming the coolant and injecting fuel at later timings reduced PN emissions during warmup and cold transient conditions. Additionally, experiments using fuel blends with different oxygenate contents showed that the chemical composition of the fuel strongly influences particulate formation under steady state and transient conditions, and that this effect is load-dependent.

Overall, the results obtained in this work indicate that wall wetting is the dominant cause of particulate formation inside the cylinder and that fuel-wall interactions involving the piston, cylinder walls, and valves during fuel injection account for a significant proportion of PN emissions in the engine raw exhaust.

Keywords: Gasoline Direct Injection, Particulate Number, Alternate fuels, PM, Load transients

## LIST OF PUBLICATIONS

This thesis is based on the work contained in the following publications:

- Paper I** Etikyala, S., Koopmans, L., & Dahlander, P. "Particulate Emissions in a GDI with an Upstream Fuel Source" in *WCX<sup>TM</sup> 19: SAE world congress experience, Detroit, MI, US*, <https://doi.org/10.4271/2019-01-1180>
- Paper II** Etikyala, S., Koopmans, L., & Dahlander, P. "Effect of Renewable Fuel Blends on PN and SPN Emissions in a GDI Engine", in *20: SAE Powertrains, Fuels & Lubricants Meeting*, <https://doi.org/10.4271/2020-01-2199>
- Paper III** Etikyala, S., & Dahlander, P. "Soot Sources in Warm-Up Conditions in a GDI Engine", *WCX<sup>TM</sup> 21: SAE World Congress Digital Summit*, <https://doi.org/10.4271/2021-01-0622>
- Paper IV** Etikyala, S., Koopmans, L., & Dahlander, P. "History Effect on Particulate Emissions in a Gasoline Direct Injection Engine", in *SAE Int. J. Engines 15(3):445-455, 2022*, <https://doi.org/10.4271/03-15-03-0999>
- Paper V** Etikyala, S., Koopmans, L., & Dahlander, P. "Visualization of soot formation in load transients during GDI engine warm-up", under review in *International Journal of Engine Research*.

Other contributions and publications not included in this thesis:

- Paper VI** Melaika, M., Etikyala, S., and Dahlander, P. "Particulates from a CNG DI SI Engine during Warm-Up", *WCX<sup>TM</sup> 21: SAE World Congress Digital Summit*, <https://doi.org/10.4271/2021-01-0630>
- Paper VII** Dahlander, P., Babayev, R., Ravi Kumar, S., Etikyala, S. et al. "Particulates in a GDI Engine and Their Relation to Wall-Film and Mixing Quality", in *WCX<sup>TM</sup> 22: SAE world congress experience, Detroit, MI, US*, <https://doi.org/10.4271/2022-01-0430>



## ACKNOWLEDGEMENTS

The amount of efforts put forward by our generation to keep the natural resources in a good state for the upcoming generations is not to be taken lightly. I am humbled and honored to contribute through my doctoral thesis work. I would first like to thank my supervisors, Prof. Petter Dahlander and Prof. Lucien Koopmans, for giving me this opportunity to work on such an interesting topic. The two of you have always kept me motivated by providing numerous opportunities for a challenge. Especially Petter, who not only designed the in-house controller, vital for the later part of the thesis but also has an open office policy where we could discuss any topic without prior notice. Some of our discussions also included going over recipes of Asian dishes and figuring out the right temperatures to cook them. I sincerely appreciate him providing the space for open communication.

I would also like to thank Prof. Ingemar Denbratt for providing the opportunity to work on this project, and the Combustion Engine Research Centre (CERC) for financial support. I thank Associate Prof. Jonas Sjöblom and Dr. Timothy Benham for sharing their expertise and helping with the measurement equipment. I am also hugely grateful to Alf hugo, Robert, Patrik, and Anders for always willing to help me. I extend my gratitude to Arjan Helmantel, amongst others from Volvo Cars and Anna Karvo from NESTE for offering support with alternative fuels.

Countless people have been tremendously engaging, patient and friendly catering to a supportive working environment at work. Coming from aerospace engineering background, internal combustion engines were intimidating at first. But the introduction course by Prof. Sven Andersson was a gem in itself in paving the way for new-comers. Thanks Sven, also for our occasional språk-cafe moments in Swedish, which I still use as proof of me learning Svenska. Thanks Elenor Norberg and Blagica for the administrative help. I am also grateful to all my colleagues, specially Vignesh, Magnus, Andreas, Mindaugas, Michael, Jelmer, Marco, Pratheeba, Josefine, Kristoffer, Akichika and Jayesh for making me aware of the world that lies outside my own experiences. I extend my gratitude to my office mates, Jiayi and Zhiqin for their counsel and support in tough times. To the PhD students who are yet to finish - Nidal, Abhilash, Mohammad and Victor, remember this too shall pass and thank you for being so kind.

Finally, a heartfelt thanks to my family, Mom, Dad and my dearest grandma for their sympathetic ear, persistent support and love. Special mention to my brother, Vedavyas who has even taken up a PhD of his own to relate to my problems. Lastly but most importantly, I thank Vamshi, who has provided endless support as I have deliberated over my concerns and provided many happy distractions to help me rest my mind outside of my research. He even made me an easel when I merely mentioned painting. How much he regrets doing that is another thing now. I'm so excited to meet our new family member in this upcoming next chapter, here's to you little baby!





*to my mom*



# Contents

Abstract	i
List of publications	iii
Acknowledgements	v
List of Acronyms	1
<b>I</b> Introductory chapters	<b>3</b>
<b>1</b> Introduction	<b>5</b>
1.1 Motivation	5
1.2 Objectives and Research Questions	9
1.3 Approach and Thesis Outline	13
<b>2</b> Background	<b>17</b>
2.1 Particulates from GDI engines	17
2.1.1 Cold Starts	17
2.1.2 Transients	18
2.1.3 High Loads	20
2.2 Particle formation mechanisms	21
2.2.1 In-cylinder mechanisms that cause particulate formation	21
2.2.1.1 Spray interactions	21
2.2.1.2 Mixing quality	22
2.2.1.3 Injector tip-wetting	22
2.2.1.4 Particulates from Oil	23
2.3 PN measurements	24
2.3.1 Interpreting particulate size distribution graphs	24
2.4 Current techniques for PN reduction	25
2.4.1 Injection pressure tuning	25
2.4.2 Optimizing injection timing	26
2.4.3 Split Injection and Multiple Injection	27
2.4.4 Optimization of Spray targeting	27
2.4.5 Gasoline Particulate Filters	27

2.4.6	Renewable fuels . . . . .	28
2.4.7	Role of alternative fuels at cold starts . . . . .	29
<b>3</b>	<b>Experimental Setup and Methods</b>	<b>31</b>
3.1	Engine . . . . .	31
3.1.1	Naturally aspirated metal engine and operating conditions . . . . .	32
3.1.2	Metal cylinder head with optical access . . . . .	36
3.1.3	Pre-conditioning of the engine and the measurement system for investigation of history effects . . . . .	36
3.1.4	Procedure for visualizing soot sources during load transients . . . . .	39
3.2	Measurement Setup . . . . .	42
3.2.1	DMS500 . . . . .	42
3.2.2	Thermodenuder . . . . .	43
3.2.3	Methodology for image analysis . . . . .	45
<b>4</b>	<b>Summary of publications</b>	<b>47</b>
4.1	Paper I . . . . .	47
4.2	Paper II . . . . .	48
4.3	Paper III . . . . .	49
4.4	Paper IV . . . . .	50
4.5	Paper V . . . . .	51
<b>5</b>	<b>Results and Discussion</b>	<b>53</b>
5.1	Particulate emissions and measurements . . . . .	53
5.1.1	Investigation of PN in GDI with an upstream injector . . . . .	53
5.1.2	PN and oxygenated fuel blends . . . . .	57
5.2	Particulate formation and visualization . . . . .	60
5.2.1	Identification of soot sources during warm-up . . . . .	60
5.2.2	History effect of soot formation on PN emissions . . . . .	63
5.2.3	Visualization of soot sources during cold transients . . . . .	68
5.2.4	Effect of fuel on PN during load transients . . . . .	73
<b>6</b>	<b>Conclusions</b>	<b>75</b>
6.1	Novelty of the Research . . . . .	78
<b>7</b>	<b>Outlook and future work</b>	<b>79</b>
	<b>Bibliography</b>	<b>81</b>
	<b>List of Figures</b>	<b>87</b>
	<b>List of Tables</b>	<b>90</b>
<b>II</b>	<b>Appended Papers</b>	<b>91</b>



# List of Acronyms

AFR	-	Air to Fuel Ratio
BC	-	Black Carbon
Ca	-	Calcium
CAD	-	Crank Angle Degrees
CADbTDC	-	CAD before TDC
CO <sub>2</sub>	-	Carbon dioxide
CoV	-	Coefficient of Variance
CS	-	Catalytic Stripper
DI	-	Direct Injection
DOE	-	Design of Experiments
DPF	-	Diesel Particulate Filter
E10	-	Gasoline + 10% (v/v) Ethanol
E15	-	Gasoline + 15% (v/v) Ethanol
E5	-	Gasoline + 5% (v/v) Ethanol
EN228	-	European Standards for gasoline (EN 228)
ETBE	-	Ethyl Tert-Butyl Ether
EtOH	-	Ethanol
EU	-	European Union
GDI	-	Gasoline Direct Injection
GPF	-	Gasoline Particulate Filter
IMEP	-	Indicated Mean Effective Pressure
lpm	-	Litres per minute
MBT	-	Maximum Break Torque
MFB50	-	50% Mass Fraction Burnt
Mg	-	Magnesium
NEDC	-	New European Driving Cycle
P	-	Phosphorus
PFI	-	Port Fuel Injection
PLS	-	Partial Least Squares
PM	-	Particulate Mass
PMP	-	Particle Measurement Program
PN	-	Particulate Number
R83	-	Regulation no. 83
RDE	-	Real Driving Emissions
S	-	Sulphur
SI	-	Spark Ignition
SMPS	-	scanning mobility particle sizer
SOI	-	Start of Ignition
SPN	-	Solid Particulate Number
SVOC	-	Semi Volatile Organic Compound
TD	-	Thermodenuder
TDC	-	Top Dead Centre
TWC	-	Three Way Catalyst
UNECE	-	United Nations Economic Commission for Europe

Part I  
Introductory chapters





# 1 Introduction

## 1.1 Motivation

Internal combustion engines are widely used in transportation due to their high efficiency and reliability, and have played a major role in shaping both public lifestyles and the global economy over the 150 years since they were first developed. Unfortunately, their increased usage in the automotive sector and elsewhere has a disadvantage in terms of emissions. Particulate emissions due to road transportation have attracted particular interest and concern in recent years because several medical studies have shown that that particulates can adversely affect human health [1, 2]. For instance, particulates in inhaled air enter the lungs and then pass through to the circulatory system via the alveoli [2, 3, 4]. Therefore, in addition to their contributions to air pollution and global warming, vehicular emissions can cause significant health and environmental problems.

Over 25% of all ultrafine particulates emitted into the atmosphere originate from road transportation, with major vehicular sources including internal combustion engines, brakes, and sometimes also tires as shown in Figure 1.1. Because particulates are a public health hazard, stringent regulations on their emissions have been introduced [5]. The need to reduce particulate emissions has motivated extensive research on control mechanisms for internal combustion engines and improvements in engine technology [5, 6].

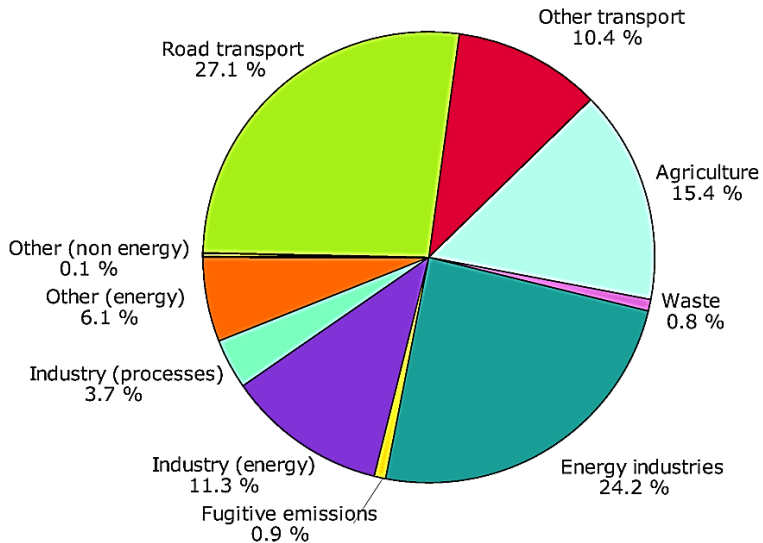


Figure 1.1: *Sector split emissions of primary and secondary fine particulate emissions by particulate mass (PM10) [Source: EAA 18]*

Gasoline engines use a pre-mixed combustion process that produces less soot than similarly powerful diesel engines that rely on diffusion combustion. This is particularly true for modern port fuel injection (PFI) engines, which achieve excellent mixture quality under stationary operating conditions. Since their introduction in 1996, gasoline direct injection (GDI) engines have been widely adopted by automotive manufacturers because of their high efficiency. Most GDI engines operate using a stoichiometric air/fuel mixture formed by injecting the fuel early during the intake stroke. GDI engines are a key enabler for reducing CO<sub>2</sub> emissions from gasoline-powered vehicles because they have higher compression ratios and lower charge temperatures than Port Fuel Injection (PFI) engines, leading to higher volumetric efficiencies and lower fuel consumption.[7, 8]. Because of these benefits and the potential for further reductions in fuel consumption and emissions, there is strong interest in developing improved GDI engines, despite their greater cost compared to PFI engines. GDI engines also have the potential to deliver considerable reductions in emissions during cold starts by avoiding the formation of liquid fuel films on the intake port walls [9]. However, particulate emissions from GDI engines tend to exceed those of PFI engines under standard operating conditions due to the formation of fuel-rich zones and wall-wetting.

Techniques such as exhaust after-treatment, recirculation of exhaust gas into the cylinder, and fuel reformulation to increase oxygenation have been used to reduce soot emissions [10, 11]. For instance, Gasoline Particulate Filter (GPF)s are widely used to capture soot from engine exhaust [12]. Current GPFs are less efficient at removing soot than Diesel Particulate Filter (DPF)s, but research efforts aiming to improve their performance are ongoing. Pressure build-up in the exhaust manifolds of vehicles can be avoided by periodically regenerating GPFs. Unfortunately, expensive GPFs will impose increased costs: they increase fuel consumption by raising the engine's backpressure and may also increase maintenance costs if they must be replaced frequently [13]. Active regeneration would require the use of lean air-fuel mixtures at certain high (but not too high) temperatures and may be essential when using exhaust aftertreatment systems containing catalysts. DI fuel injection systems tend to produce less homogeneous fuel-air mixtures at ignition than PFI systems because direct injection reduces mixing times and may cause fuel impingement on the combustion chamber and cylinder walls, the piston, or the valves. This leads to the formation of fuel-rich regions and cyclic variation, both of which tend to increase soot formation [14, 15, 16]. Particulate formation in gasoline engines is usually attributable to inadequate air-fuel mixing [9]. Increasing mixture homogeneity in SI engines generally improves combustion quality, which is essential for minimizing particulate emissions. Because particulate emissions from GDI engines depend on many different factors whose relationships are poorly understood, research is needed to clarify the processes that control mixture homogeneity and particulate formation/degradation in order to guide the development of robust strategies to minimize particulate emissions.

Alternative fuels for gasoline direct injection engines have also drawn a lot of attention recently. Recent studies have shown that particulate formation and emissions from GDI engines can be reduced by replacing some part of conventional fossil gasoline with alternatives such as Ethanol (EtOH), methanol, butanol, or methane. Several

alternative fuel blends for spark ignition engines are widely available, and gasoline containing 5% ethanol by volume (E5) is now common in Europe (European Committee for Standardization 2008). Gasoline + 10% ethanol by volume (E10) blends are also ubiquitous, and gasoline + 15% ethanol by volume (E15) has entered the market for newer vehicles in the USA (U.S.C. §7546).

Table 1.1: EU emissions standards for particulate emissions from GDI-powered vehicles.

<b>Emissions</b>	<b>Units</b>	<b>Euro 5a</b>	<b>Euro 5b</b>	<b>Euro 6b</b>	<b>Euro 6c</b>	<b>Euro 6d</b>
		Jan 2009	Jan 2013	Sept 2015	Sept 2018	Jan 2021
<b>PM</b>	mg/km	5	4.5	4.5	4.5	4.5
<b>PN</b>	#/km	-	-	$6.0 \times 10^{12}$	$6.0 \times 10^{11}$	$6.0 \times 10^{11}$

Table 1.1 shows how the legally mandated upper limit on particulate emissions from GDI engines has fallen in recent years. Engine-out Particulate Mass (PM) emissions can be controlled relatively easily by using a GPF to remove larger particulates, but PN emissions are dominated by smaller particles that are less readily removed. Consequently, a GPF can only reduce PN emissions by 60-80%, which is insufficient to ensure compliance with future regulations, especially given that future regulations will apply to particles with smaller diameters than is currently the case. We therefore cannot assume that current technologies will be sufficient to ensure compliance with future regulations. New ways of reducing particulate formation during engine operation are thus needed to reduce engine-out particulate emissions to a level that allows the remaining particles to be removed with a GPF while minimizing the filter’s size without a significant reduction in pressure.

## Particulate emissions in GDI engines

Historically, most gasoline engines have used PFI systems, but GDI engines have become more popular in recent years because GDI facilitates engine downsizing, reduction of emissions, and significant improvements in operating performance. Improving the design of GDI engines requires a deep knowledge of the processes occurring during an engine cycle. In particular, a thorough understanding of the injection process is needed because it influences all subsequent events in the engine cycle including air/fuel mixture formation, combustion, and emissions formation. The gasoline jet breakup modality and the distribution of the fuel spray within the combustion chamber are key factors in mixture formation that strongly affect both combustion quality and emissions. The relatively small dimensions of the combustion chamber and the speed of the fuel jet mean that spray-wall impacts leading to the formation of liquid wall films can be difficult to prevent. However, avoiding such wall impingement is seen as a key requirement for achieving clean combustion, reducing fuel consumption, and lowering emissions. These considerations, first raised years ago, prompted extensive mathematical modelling and experimental characterization of fuel jet behaviour and wall impingement, and work in this area is ongoing.

The processes of mixture formation and combustion and the formation and emission of pollutants have been analysed in detail. It is well established that mixture formation is sensitive to various operating and design parameters of the engine including the injection pressure, fuel temperature, combustion chamber geometry, injection strategy, and ignition timing [11]. Moreover, as mentioned previously, PM emissions from GDI engines tend to be substantially higher than those from comparable PFI engines [10], prompting extensive efforts to reduce PM formation. Research in this area has shown that understanding soot formation mechanisms and optimizing thermodynamic processes, engine design parameters, and the composition and physical properties of fuels are all essential for minimizing particulate emissions [10, 6]. Higher injection pressures tend to reduce both PN and PM formation by promoting the formation of more homogeneous air-fuel mixtures and more efficient fuel vaporization [17]. Injection and combustion (homogeneous or stratified) strategies also strongly affect particulate emissions [18]. Consequently, there is great interest in multi-phase injection strategies that make it possible to achieve a low fuel jet length while improving mixture formation and reducing the likelihood that fuel will impinge on surfaces, all of which tend to reduce particulate emissions [19]. Another interesting strategy for reducing particulate emissions is to use fuel blends with reduced contents of aromatic and olefin components to improve mixture formation and combustion [6]. Adding ethanol to gasoline reduces the fuel's vapor pressure and promotes evaporation, thereby reducing particulate formation [20, 21]. Deposition and fouling are also important processes, especially in GDI engines where the injection system is in direct contact with the combustion gases and exposed to high temperatures and pressures. Significant injector fouling can lead to engine misfiring and elevated PN levels in the exhaust[6].

## **Particulate formation in GDI engines**

Liquid fuel impingement on the piston top has been identified as a major factor causing high PN emissions. Accordingly, preventing such impingement can reduce emissions by more than an order of magnitude [22]. Furthermore, researchers have found that PN emissions are relatively insensitive to cam phasing and spark timing, especially at high engine loads [23], and one study found that PN emissions from a GDI engine during the Federal Test Procedure urban driving cycle (FTP 75) were higher under lean conditions than under stoichiometric conditions [14]. Specifically, although lean operation reduced fuel consumption, it increased the formation of small particulates. The injection system also significantly affected both PM and PN emissions, and it was found that particulate emissions were minimized by using a high injection pressure and stoichiometric conditions.

This thesis focuses on PN emissions from GDI engines in order to facilitate the development of new engine designs that can comply with future emissions standards. Specifically, the work presented investigates sources of PN formation during engine warm-up, which have received limited attention in previous studies, and the effects of varying the coolant and oil temperatures on PN emissions and associated processes. Engine experiments were conducted at high engine speeds to ensure stable operation with a fast warm-up process.

## 1.2 Objectives and Research Questions

This thesis presents research conducted within the framework of the *Towards Zero Emissions in GDI engines* project which is funded by Combustion Engine Research Centre(*CERC*). Its overall goal was to identify, isolate, and study particulate formation mechanisms in GDI engines in order to gather knowledge that will facilitate the development of tools to reduce PN emissions from GDI engines. More specifically, the work presented herein was conducted to identify the mechanisms governing soot formation in a homogeneous SI engine and to develop strategies for minimizing this soot formation. Figure 1.2 outlines the scope of the project and the work that was done within it.

During the first phase of the project, PN emissions from GDI engines were investigated. Unlike other engine emissions, particulate emissions are sensitive to many factors. Consequently, there are several possible ways to reduce PN emissions. The first phase of the project therefore aimed to quantitatively compare reported strategies for reducing PN emissions while also evaluating the relative importance of different particulate formation mechanisms. It was found that wall wetting was the dominant mechanism of PN formation and that its contribution to overall PN emissions was large enough to mask the contributions of all other PN formation mechanisms under almost all driving conditions.

One finding from the first experimental campaign measuring PN emissions from GDI engines was that PN emissions were highest at higher engine loads that increase the likelihood of wall-fuel interaction. Additionally, during the first campaign it was observed that over 90% of particulates emitted from the engine consisted mostly of volatile organic compounds (VOCs). Increasing the injection pressure increases the momentum of the fuel droplets, which in turn increases the penetration length of the fuel spray and the likelihood that the spray will impinge on the surface of the piston. The likelihood and extent of wall-fuel interaction also depends on the injection duration and injection timing. The net effect of these factors on PN emissions is considered in Paper 2. In addition, alternative fuels for gasoline are also tested for their ability to reduce PN at all driving conditions to provide a comprehensive report. Using renewable oxygenates in gasoline blends gave deeper insights on how easy it is for one to use them and avoid a lot of PN while driving in an urban area. The impact of blend composition on engine performance and emissions was studied experimentally using a Volvo single cylinder gasoline engine.

In phase II of the project, an endoscope was installed in the cylinder head of the metal test engine enabled optical visualization of the combustion cycle, providing remarkable insights into soot formation and the locations where it occurs. Such optical visualization is generally achieved by replacing a metal cylinder or piston with a glass or quartz alternative. Paper 3 summarizes the findings concerning the location of soot sources during engine warm-up and the resulting insights into the dominant mechanisms of PN formation in GDI engines.

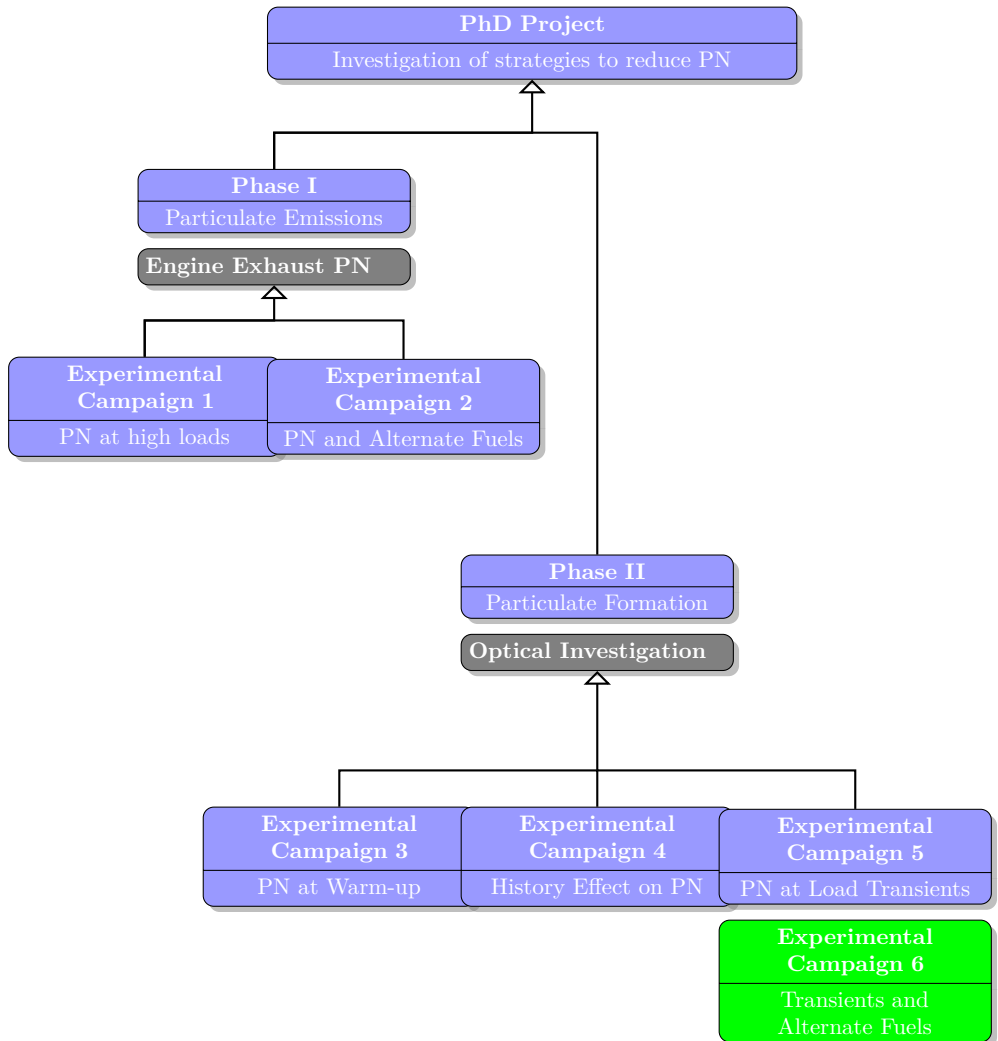


Figure 1.2: *Scope of research work in this thesis*

As stated previously, the work presented in this thesis involved measuring PN emissions and visualizing events inside the cylinder during engine operation to find ways of making GDI engines cleaner by reducing particulate emissions to zero during the most troublesome parts of a drive cycle so as to ensure compliance with current and future emissions standards. Papers 1 and 2 focused on particulate formation at high load, while Paper 3 examines cold starts and engine warm-up, revealing that the temperature of the engine's coolant significantly affects particulate formation and that delayed injection timings can reduce PN emissions.

The final set of experiments presented in this thesis examined PN formation by using an endoscope to visualize events inside the cylinder during load transients. Transients are fast-paced events that occur over a period of a few seconds, making it difficult to study their effects on engine performance and emissions. However, the use of a novel NI cRIO controller built in-house made it possible to control the engine's operation with cycle-to-cycle accuracy. Using this advance, Paper 4 introduces the concept of history effects to qualitatively describe the impact of past events on emissions during a particular transient. The new controller was also used to study cold transients, as described in Paper 5. These experiments revealed that varying the injection timing alone is not sufficient to negate the effect of the coolant temperature during fast-paced events like load transients. Additionally, the results obtained demonstrated that correlating endoscope images with tailpipe PN measurements can provide deep insights into the mechanisms controlling PN formation. A final campaign whose results are currently unpublished examined the effects of alternative fuels on PN formation during load transients.

## Research Questions

Based on the issues outlined above, this thesis aims to answer five research questions:

- Does the use of dual injection systems to control the homogeneity of the charge mixture help reduce PN formation?
- What are the benefits of increasing the fuel's oxygen content in terms of PN formation and emissions?
- Can any insights useful for reducing PN emissions be obtained by locating sources of soot during engine warm-up?
- Is there any history effect on PN formation and emissions?
- Can any of the control mechanisms developed to date help reduce soot formation during load transients



### 1.3 Approach and Thesis Outline

Reducing the emissions of pollutants, and particularly soot particles, from internal combustion engines is one of the greatest challenges facing car manufacturers today. Although modern GDI engines have relatively low particulate emissions during steady state operation under near-stoichiometric conditions, they can produce and emit particles with diameters below 100 nm. These particles are regarded as both pollutants and health hazards because of their ability to enter the human circulatory system via the lungs. The research presented in this thesis was conducted to find ways to help manufacturers comply with increasingly stringent emissions standards and reduce overall PN emissions from GDI engines. Previous studies have shown that PN emissions can be reduced by using new injectors, high injection pressures, and optimal injection timings, and by avoiding transients that generate diffusion flames [6]. However, the dominant sites and mechanisms of particle formation in GDI engines remain largely unknown. The work presented in this thesis therefore used a systematic approach to isolate different mechanisms of soot formation and the factors influencing them in order to evaluate their relative importance. The results obtained were then compared to previously reported results and measurements of PN emissions. In a typical GDI engine drive cycle, most PN emissions occur during cold starts, periods of high load, and transients. This work therefore focuses on these operating conditions when seeking to identify dominant soot formation mechanisms and potential control strategies for reducing PN emissions.

Particulate emissions from gasoline engines have been studied extensively but unfortunately these studies have yielded few insights into the sources and sites of soot formation [11]. However, research on the composition and morphology of soot has shown that it consists mainly of carbon [12]. The problem of reducing particulate emissions can thus be recast as a problem of reducing the amount of carbon in the cylinder that can be transformed into soot. This can be achieved by ensuring efficient combustion and improving control of in-cylinder soot formation mechanisms. PN emissions have both solid and volatile components, the latter of which consist primarily of VOCs. Preliminary experiments showed that these VOCs could be efficiently removed from exhaust samples using a thermodenuder. The alternative fuels used in the study have a higher content of oxygen and a lower content of carbon than gasoline, which reduces overall soot production. Efforts to use such fuels to reduce PN emissions from GDI engines have been reported previously, with conflicting results [20]. However, there have been no comprehensive studies on the effects of alternative fuels on PN emissions under different engine conditions. Systematic experiments using oxygenated fuels were therefore conducted, revealing a load-dependent soot reduction.

Cold starts are well known to cause extensive liquid fuel deposition and incomplete combustion, resulting in high soot formation. Several recent studies have therefore investigated the benefits of pre-heating the coolant before starting the engine to alleviate these problems. A novel contribution in this area was made by identifying the dominant soot sources as the engine goes through different stages of warm-up, from cold to completely warm, revealing ways of minimizing piston impingement at low loads. In addition, the

use of a new controller to achieve consistent cycle-to-cycle control over engine parameters with CAD resolution made it possible to correlate endoscope images with tailpipe PN emissions, revealing for the first time that engine operating conditions in the recent past can strongly influence current PN emissions. This phenomenon has been designated the “history effect”. In addition to demonstrating the history effect, the studies presented herein show how consistent they are and how far back in time they can extend. Load transients are another under-explored phenomenon with significant effects on PN emissions from GDI engines. While some studies have examined transients in GDI engines [10, 24, 25, 26], these events are so short that it is impossible to fully capture their behaviour just by measuring emissions. To overcome this problem, a new controller was designed in-house to provide cycle-to-cycle control over the throttle, injection duration, timing, and ignition control in a metal engine. This made it possible to obtain detailed visualizations of soot formation in the cylinder during transients and to characterize its development with CAD precision.

As the above discussion shows, few previous studies have examined PN and soot formation during individual short-lived events within a drive cycle, and those that have been reported have focused exclusively on one or the other rather than looking at both simultaneously. The work presented herein therefore has significant novelty because it includes experimental studies on particulate emissions and combustion behaviour during complex engine events such as load transients. Moreover, it shows that combining optical visualization with PN measurements can provide deep insights into sources of soot formation.

## Outline

This thesis is organized into seven chapters. The current chapter provides an overview of the problems caused by particulate emissions from GDI engines and the contribution of the automotive sector (and passenger cars in particular) to greenhouse gas emissions and public health hazards. It also outlines the problems facing the automotive industry as it strives to reduce the PN emissions of new vehicles. These two factors constitute the motivation for reducing particulate emissions from GDI engines to zero. The work presented in the subsequent chapters describes efforts made to achieve this goal and answer the research questions posed above. Chapter 2 briefly describes the origins of the particulate matter in engine exhaust, which were the focus of the first set of experimental investigations described in the thesis. Key publications and theoretical considerations pertaining to fuel injectors, sprays, and mixture formation are summarized, and the history of GDI technology is briefly reviewed. Chapter 2 also introduces the complications caused by the presence of multiple soot sources in an engine and their effects on emissions. Both cold starts and engine warm-ups are discussed with reference to previous literature. Chapter 3 presents the apparatus and methods used in the two experimental campaigns. It also includes a discussion of the methods used to correlate endoscope images of events inside the cylinder with tailpipe emissions, which were used to evaluate the potential benefits of different strategies for restricting PN emissions from GDI engines. Chapter 4 briefly summarizes the appended publications on which this thesis is based. Chapter 5 presents and discusses the main findings of the experimental campaigns and appended publications. Chapter 6 summarizes the conclusions drawn from the presented work and presents answers to the research questions posed in section 1.2. Finally, Chapter 7 proposes some future research directions that could build on the work presented herein and summarizes the lessons learned during this research work.



## 2 Background

The introduction of GDI was a major advance in the development of gasoline engines because of its potential to reduce CO<sub>2</sub> emissions while also improving torque and power output. To exploit these advantages, direct injection is often implemented in downsized turbocharged engines. GDI also enables more precise control over fuel injection than PFI, potentially enabling greater thermal efficiency and superior fuel economy [27] while also delivering a higher specific power output than comparable PFI engines [28]. However, the PN emissions of GDI engines are higher than those of conventional PFI engines. In fact, a car with a GDI engine without particle filters emits significantly more harmful particulates than a diesel engine with a particle filter. This is highly problematic because many studies have shown that respiratory intake of aerosol particles in the ultrafine size range (diameter <100 nm), which constitute the majority of particulate emissions from GDI engines [29, 30, 31, 32, 33], can have severe adverse health effects. Among other things, exposure to such particulates has been linked to pulmonary inflammation, asthma, and cardiovascular conditions. Consequently, regulations on particulate emissions are expected to become more stringent and to impose limits on emissions of particles with diameters down to 10 nm for all new vehicles [30]. Complying with these requirements will be challenging for vehicle manufacturers and will require a deeper understanding of the mechanisms of PN formation and sources of PN emissions from GDI engines.

### 2.1 Particulates from GDI engines

To fully understand the particulate emissions from GDI engines, it is important to consider real driving emissions (RDE) in a typical drive cycle. Figure 2.1 shows the variation in PN emissions from 1.6 L GDI and PFI engines over the New European Driving Cycle (NEDC) [10]. As shown in the plot, there are three key phases of the drive cycle during which PN emissions from the GDI engine are particularly high:

- **cold starts/engine warmup,**
- **transients,** and
- **high loads.**

#### 2.1.1 Cold Starts

Particle number emissions from GDI engines are significantly higher during cold starts than after the engine has warmed up to its normal operating temperature. Consequently, cold starts contribute significantly to overall PN emissions [12]. During a cold start, the heat transfer from the combustion chamber surface to the air-fuel mixture is considerably reduced, which reduces the rates of fuel vaporization and mixing. This in turn leads to the formation of a heterogenous charge with localized fuel-rich regions [11]. Cold-start particulate emissions account for more than half of the total PN emissions from a GDI engine over a drive cycle [10].

Many studies have investigated the particulate emissions of GDI engines during cold starts. Notably, studies examining cold starts from  $-10\text{ }^{\circ}\text{C}$  [34] and engine warm-ups from  $40\text{ }^{\circ}\text{C}$  [35] both found that PN concentrations and the sizes of the emitted particles decreased as the engine warmed up. These studies also indicated that the engine coolant temperature strongly influences combustion and thus PN formation. Other investigations have shown that particulate emissions are heavily dependent on the properties of the fuel including its aromatic content, volatility, and oxygen content [1], and it has been suggested that the vapor pressure and structure of the fuel can influence particle formation [36]. Finally, PN emissions were found to be highly sensitive to engine operating and thermal conditions [22].

The effects of some primary engine parameters on PN emissions have been investigated in efforts to identify optimal strategies to reduce them. Parameters examined frequently in this context include the temperatures of the engine oil and coolant, the spark or ignition timing, the fuel injection pressure, and the start of injection (SOI) timing. A study on the effect of coolant temperature on particulate emissions from a GDI engine found that total PN and PM emissions decreased as the coolant temperature increased, and fell dramatically once the coolant temperature rose above  $70\text{ }^{\circ}\text{C}$  [35]. Another group observed a similar decrease with increasing coolant temperature and concluded that the fuel spray dispersed more widely under warmer conditions, thereby improving mixture homogeneity and combustion stability [1]. Separately, Price et al. [34] reported that PN emissions from GDI engines were high under cold start conditions and decreased as the engine warmed up. Finally, Fu et al. [37] found that more particulates were formed under cold-engine conditions during the first 200 s of the NEDC than during a warm-start NEDC, and linked this result to the combustion of inhomogeneous air-fuel mixtures during cold starts.

Another important factor affecting vehicular emissions is the ambient temperature. Ramadhas et al. [38] found that the proportion of particles in the 50-200 nm size range fell significantly as the ambient temperature increased from  $10$  to  $45\text{ }^{\circ}\text{C}$ . Additionally, Mamakos et al. [39] showed that particulate emissions during the NEDC driving cycle doubled upon reducing the ambient temperature from  $+22$  to  $-7\text{ }^{\circ}\text{C}$ . In contrast, both Mamakos et al. [39] and Mathis et al. [40] found that the ambient temperature had only a limited impact on particulate emissions during the Common Artemis Driving Cycle (CADC). However, Fushimi et al [41] found that particulate emissions from a GDI engine during the Japanese JC08 cycle under hot start conditions at an ambient temperature of  $5\text{ }^{\circ}\text{C}$  were three times those observed at an ambient temperature of  $35\text{ }^{\circ}\text{C}$ .

### 2.1.2 Transients

During load transients in a GDI engine, there is a sudden change in the fuel mass injected into the cylinder that causes abrupt changes in PN emissions. The increased fuel intake leads to extensive wall-wetting and the emergence of fuel-rich zones that increase soot formation. It also affects homogeneity of the fuel-air mixture, again favouring soot formation. The increased load may even cause pool fires before steady state conditions are restored, leading to further particulate formation [34]. The air-fuel ratio (AFR) is a key

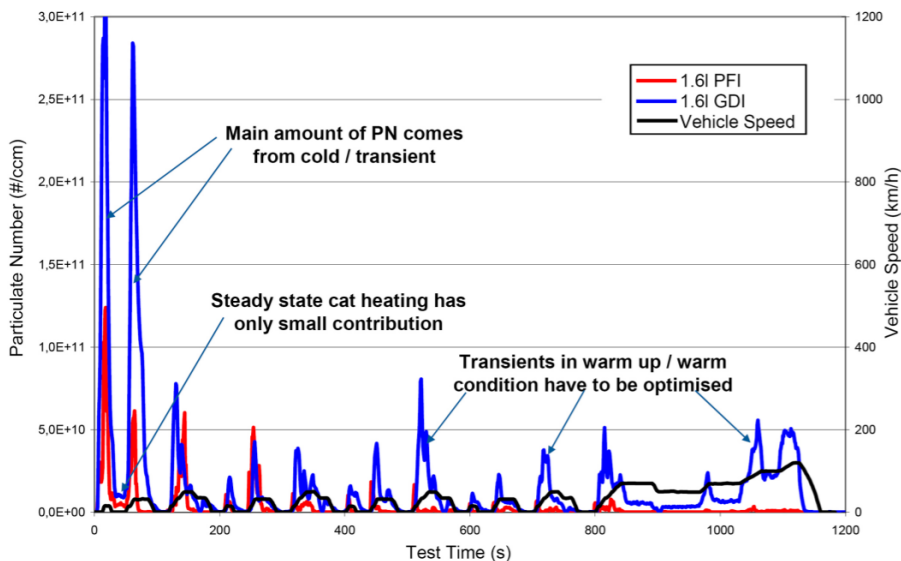


Figure 2.1: *The NEDC drive cycle test sequence and the associated PN emissions from PFI and GDI engines with equal swept volumes. PN emissions are particularly high during cold starts, engine warm-up, transients, and high load drive phases [10].*

determinant of PN emissions: rich and stoichiometric AFRs give substantially higher PN emissions than lean AFRs (by up to an order of magnitude in many cases), which becomes particularly important during engine transients. Moreover, alcohol-containing fuels exhibit poor vaporization during load transients, which again reduces mixture homogeneity and thus increases soot formation.

Perhaps the most important parameter in terms of emissions is the cold start temperature, especially in cases where the engine is started while cold and immediately revved up to a high load in order to keep combustion going, resulting in a cold transient. Several studies have shown that the lower the start temperature, the higher the particulate emissions [10, 42, 43]. For example, Ricardo et al. [44] found that a GDI engine would generate more than  $2.5 \times 10^{13}$  particles over a WLTP cycle with a start temperature of  $-7^\circ\text{C}$  but only  $5 \times 10^{12}$  particles with a start temperature of  $23^\circ\text{C}$ . Therefore, during engine starts, it is important to increase the equivalence ratio in order to reach the engine's designed operating temperature as quickly as possible. Combustion is therefore performed under non-stoichiometric conditions. In addition, wetting will increase if the walls of the cylinders and the piston crowns are cold, leading to increased soot formation. Unfortunately, the reproducibility of particle concentration measurements during an engine cycle is limited even in steady-state studies, which makes detailed analysis of events during transient operation extremely challenging.

In a typical GDI engine drive cycle, transients involving abrupt changes in engine speed and/or load account for a substantial proportion of the total PN emissions. These sudden changes in engine parameters lead to changes in combustion that cause the engine to take some time to restore steady state operation, which is reflected in the PN emissions. The difficulty of measuring particulates in the exhaust also increases because the changes in engine parameters are sudden and it takes time for them to be reflected in the PN concentrations. Consequently, there have been few studies on particulate formation during transients. One of the studies included in this thesis aimed to overcome this problem through controlled variation of parameters with important effects on PN emissions during a predesigned simple load transient in a GDI engine. This made it easier to identify the main variables influencing these emissions in order to develop targeted strategies for their reduction.

### **2.1.3 High Loads**

In engines of all types, high loads typically necessitate the injection of a greater quantity of fuel and thus cause higher PN emissions. Fuel-wall interactions are a major cause of PN formation, and increasing the quantity of injected fuel increases the potential for such interactions. Injecting large amounts of fuel also necessitates a longer injection duration, increasing the likelihood that liquid fuel will interact directly with the piston as it moves from BDC towards TDC. This issue is exacerbated by the high fuel injection pressures used in many modern engines, which increase liquid penetration and thus increase the likelihood of liquid fuel reaching the walls or piston. Any unburnt fuel that remains in the cylinder after the end of combustion will also increase PN emissions. At relatively high loads, the tumble and turbulent kinetic energy are strong, leading to enhanced mixing. Nevertheless, achieving a completely homogeneous air-fuel mixture in direct injection engines can be challenging, and imperfect homogenization may cause the presence of fuel-rich regions in the mixture, favouring soot formation. The fuel spray may also be deflected by strong tumble motion, further reducing mixing quality.



## 2.2 Particle formation mechanisms

Particle formation occurs during the combustion of fuel in the combustion chamber of an internal combustion engine. The formed particles may subsequently grow via nucleation of supersaturated vapours in the exhaust gas after-treatment system [6, 11]. Particulate emissions from GDI engines include ultrafine particles that are  $< 100$  nm in size. Particles in this size class have come under intense scrutiny in recent years because of their adverse effects on human health.

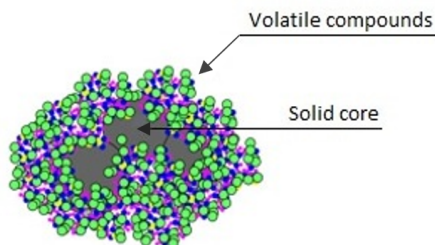


Figure 2.2: *Illustration of a typical particulate found in engine exhaust [45]*

Ultrafine particles contribute little to particulate emissions by mass but account for a large fraction of particulate number emissions. Particles emitted from engines typically have complex structures featuring a solid core that forms first and is subsequently coated with volatile compounds (see Figure 2.2). Volatiles including sulphates, nitrates, and volatile organic compounds (VOC) account for almost 90% of the mass of ultrafine particulates [14, 6, 12]. Most PN formation mechanisms contribute to the formation of both the solid core and the volatile coating.

### 2.2.1 In-cylinder mechanisms that cause particulate formation

#### 2.2.1.1 Spray interactions

Any fuel that is injected into the cylinder but not promptly vaporized will inevitably come into contact with the piston or the cylinder walls. The interactions of the fuel spray with the cylinder walls, piston, and valves contribute significantly to particle formation, so studying these interactions can provide important insights into the mechanisms by which particulates are formed. Figure 2.3 shows an image of a fuel spray being injected into the cylinder of a GDI engine with a Start of Ignition (SoI) of  $-320$  CAD before TDC (CADbTDC), which is a typical value for a GDI engine. In the figure, the fuel spray can be seen to interact with various surfaces, resulting in valve impingement, cylinder wall impingement, and piston wall-wetting. All three types of interaction are known to cause PN formation in GDI engines, although their relative and absolute importance are temperature-dependent. Fuel films on the combustion chamber wall also contribute to PN formation in GDI engines. Fuel deposited on the wall cannot be adequately mixed with air before the flame arrives and therefore forms localized fuel-rich zones with elevated levels of particulate formation [13]. Fuel film formation also dilutes the oil films on the cylinder walls that ease piston movement.



Figure 2.3: *Image of a fuel spray injected into the cylinder of a GDI engine (SOI: -320 bTDC)*

### 2.2.1.2 Mixing quality

Several factors make it impossible to form a perfect air-fuel mixture inside the cylinder. Piston wetting can generally be avoided by adjusting the SOI timing. However, the SOI timing must also be set so as to provide a mixing period long enough to enable adequate air-fuel mixing. The choice of injection timing is therefore a compromise between avoiding piston wall-fuel interactions and ensuring adequate mixing time. The formation of a very well-mixed charge would avoid these problems and thus minimize PN emissions. PFI systems allow longer mixing times than GDI systems, and therefore tend to produce more homogeneous fuel-air mixtures even when the GDI system is operated in homogeneous mode. It is possible that by combining GDI and PFI, one could retain the benefits of GDI while producing lower PN emissions than would be achieved with GDI alone.

### 2.2.1.3 Injector tip-wetting

Wetting of the injector tip is another important cause of particulate emissions in GDI engines. In endurance tests, where the engine is initially equipped with clean injectors and operated under stationary conditions for several hours, PN emissions are often observed to increase before reaching a high but stable level. Under these stabilized conditions, the injector tip surface is usually covered with a thin layer of carbon-based deposits, as shown in Figure 2.4 [15, 16]. It is assumed that this layer forms if liquid fuel remaining on the injector tip after the end of injection cannot fully evaporate before the onset of combustion; when the flame reaches this residual fuel, high temperatures and a lack of oxygen lead to the formation of particulate matter and deposits on the tip surface [46]. Deposit formation on the injector tips may also compromise spray quality because

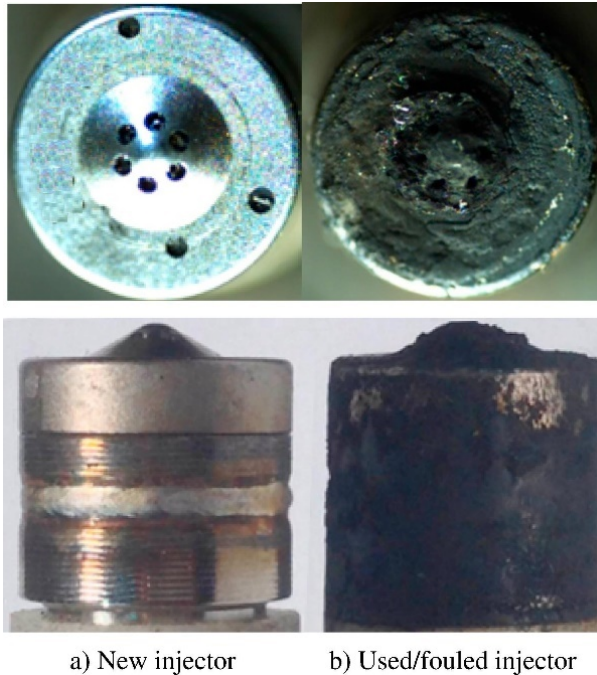


Figure 2.4: *Photographs of a GDI fuel injector before and after usage [15]*

the porous nature of the deposited material allows it to store liquid fuel and retard its evaporation, thereby accelerating further deposit growth until an equilibrium between deposit formation and removal is reached.

#### 2.2.1.4 Particulates from Oil

The engine exhaust also contains particulates originating from the engine lubrication oil (also known as engine oil, motor oil, and engine lubricant) that coats the piston and cylinder walls. The desorption of Semi Volatile Organic Compound (SVOC)s from this coating layer during the exhaust stroke is both a major pathway of oil loss and an important contributor to PM emissions [47]. It is well-known that lubrication oil is continually consumed in the combustion chamber. Although its rate of consumption in modern engines is low – values of 0.2% [48] and 0.1% [49] are typical in terms of fuel consumption – it can nevertheless contribute significantly to overall particulate matter emissions [50, 51]. For example, particles derived from lubrication oil were estimated to account for almost a quarter of the total PM emissions from gasoline-powered vehicles, and PM emissions during transient operation depended strongly on the lubrication oil’s composition [51]. It was also found that the concentration of additives (Zinc (Zn), Magnesium (Mg), Phosphorus (P) and Sulphur (S)) in the lube oil correlates positively with PN emissions and that lube oils with high contents of Zn, Ca, Mg, and S were

associated with elevated PM emissions [6].

## 2.3 PN measurements

Particulate emission measurements are unfortunately highly sensitive to the choice of sampling system [5]. A robust measurement protocol using a Volatile Particulate Remover (VPR) such as that specified in the Particulate Measurement Program Particulate Measurement Program (PMP) should therefore be adopted. While several standards for measuring particles from combustion sources exist, the one most commonly used for certification in the automotive sector is in United Nations Economic Commission for Europe (UNECE) regulation no. 83 [45]. The sampling system should be able to prevent particle formation by nucleation and agglomeration downstream of the engine. As noted above, particulates have both solid and volatile components. Unfortunately, particulate measurements become highly variable when volatiles are involved because their instability can cause measurements to fluctuate widely [5].

Measuring solid particles is also challenging because engine exhaust samples must be depleted of volatiles in a way that has little or no effect on solid particles. The engine emissions at a sampling point must therefore be in a “frozen” state. Because of these difficulties, PN measurements are not always reproducible and depend strongly on the sampling system. To maximize reproducibility and enable comparisons between measurements, the sampling equipment must be kept in a constant state. Raw exhaust PN emissions from gasoline engines can be classified based on particle size: the “nucleation mode” and “agglomeration mode” comprise particles with diameters of 3-30 nm and 20-500 nm, respectively [12]. The nucleation mode accounts for almost 90% of all PN emissions but only 10% of the total particulate mass, and consists predominantly of volatiles. There are also semi-volatiles, which are defined as particles of varying size surrounding solid core particles with dimensions of 1-5 nm [52].

### 2.3.1 Interpreting particulate size distribution graphs

The particulate content of exhaust samples is quantified in terms of particle number and size distributions, which are displayed by plotting the number concentrations of particles per unit flow ( $dN/d\log D_p/cc$ ) against particle size (5 to 300 nm). Figure 2.5 shows a typical particle size distribution plot for a gasoline engine operating at a reference load point.

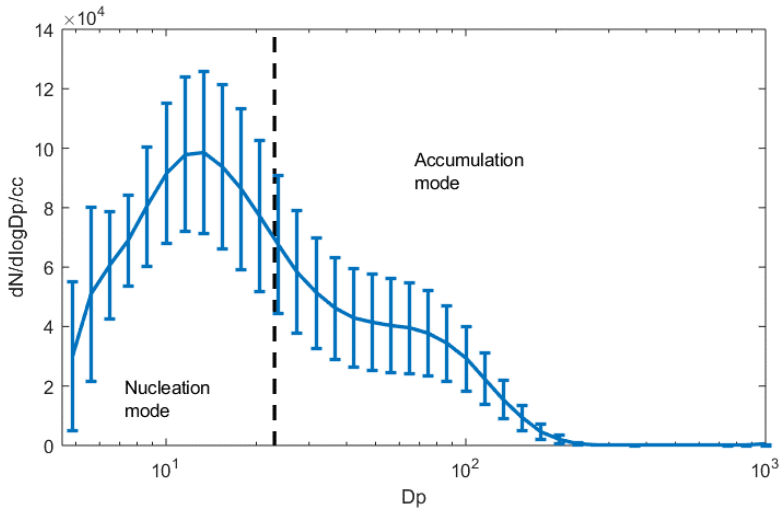


Figure 2.5: Particle size distribution for a GDI engine at a load of 5 bar IMEP and an engine speed of 1500 rpm. The dashed line indicates the regulatory limit of 23 nm for PN emissions.

## 2.4 Current techniques for PN reduction

This section briefly reviews some established solutions for reducing PN emissions from GDI engines.

### 2.4.1 Injection pressure tuning

The fuel injection pressure strongly affects PN emissions. Raising the injection pressure enhances air-fuel mixing because higher injection pressures produce smaller fuel droplets that evaporate more rapidly than larger ones. At a given load, increasing the injection pressure makes homogeneous flame front propagation faster and raises the peak pressure [53]. Higher peak pressures imply higher in-cylinder temperatures, which is beneficial for soot oxidation. The results presented in this thesis (see chapter 4 and Paper I) support the conclusion that higher pressures reduce particulate emissions, partly because they increase the momentum of fuel droplets [14]. These findings are consistent with previously reported studies on the effects of varying the injection pressure in GDI engines [8, 54, 55]. Because of these benefits, manufacturers of gasoline engines for passenger cars have begun using higher injection pressures in their engines: Volkswagen's engines operate at typical maximum injection pressure of 350 bar and others are aiming for even higher pressures such as 700 bar.

## 2.4.2 Optimizing injection timing

The injection timing in a GDI engine must be optimized to strike a good balance between achieving an adequate mixing time and avoiding piston wetting. In a GDI engine operated in homogeneous mode, fuel is injected in the intake stroke. If injection is too early, there is a risk of fuel interfering with the piston. However, if the injection occurs too late in the cycle, there will be insufficient time for mixing, resulting in poor mixture quality. Figure 2.6 shows how the PN emissions of a GDI engine vary over an SOI sweep with a fixed injection pressure. In this engine, advancing the SOI from 350 °before Top Dead Centre (TDC) to 330 °bTDC causes a dramatic reduction in PN emissions, which fall to a minimum at 270 °bTDC. This is consistent with the findings of an earlier study [56] in which pool fires were found to occur throughout the combustion process when early injection timings were used but were eliminated entirely by using later injection timings. Pool fires generate very large numbers of particulates, so to minimize PN emissions it is essential to use an SOI timing that prevents their occurrence.

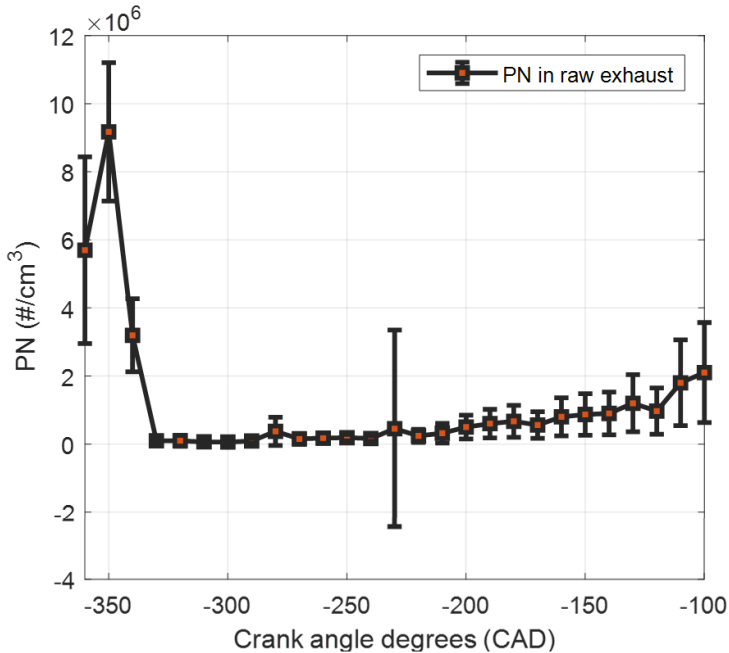


Figure 2.6: Influence of fuel injection timing (SOI) on particulate (PN) emissions at an engine load of 5 bar IMEP at 1500 rpm

### 2.4.3 Split Injection and Multiple Injection

During split injection or multiple injection operation, fuel is injected in a small sequence of injections rather than a single large injection. Because the mass of fuel injected at any one time is lower than when using a single injection strategy, the momentum of the individual fuel jets is lower. This in turn reduces the liquid penetration length and enhances the spread of the spray, leading to reduced wall-wetting and a lower spray density, both of which reduce PN emissions [53]. Split injection can also improve mixing and increase combustion stability, further reducing PN emissions.

### 2.4.4 Optimization of Spray targeting

Another way of reducing PN formation is to reduce the interaction between the fuel and in-cylinder surfaces. This can be achieved by using injectors that target the spray such that it does not directly strike the piston. However, spray optimization is not a generic solution; each spray targeting scheme is specific to a given engine type and design. Spray targeting can also ensure proper charge homogenization and thereby limit the formation of fuel films on the combustion chamber walls while increasing atomization. Recent developments have enabled improvements in spray optimization for all types of GDI engines, for instance by using side- and center-mounted injection systems.

### 2.4.5 Gasoline Particulate Filters

The density of particulates in gasoline exhausts is typically an order of magnitude lower than that in raw diesel exhaust. Therefore, a soot cake forms rapidly in diesel particulate filters (DPFs), allowing them to achieve PN filtration efficiencies of >99%. The lack of a soot cake on GPFs unfortunately leads to relatively low PN filtration efficiencies. The efficiency of a GPF during a driving cycle varies between 75 and 80% if the filter is coated, and between 45 and 50% for a non-coated filter. In both cases, the back-pressure is typically 5-10 kPa, so the filter causes only a modest increase in fuel consumption. In late October 2017, a prototype three-way catalyst with a coated GPF achieved a particulate filtration efficiency of 99%. However, the back-pressure generated by this system was very high, resulting in a significant increase in fuel consumption. Additionally, the system's filtration efficiency and back-pressure increased significantly over its lifetime, presumably because an ash layer derived from oil ash residues gradually accumulated on the filter channel wall.

## 2.4.6 Renewable fuels

Sweden wants to gradually increase renewable fuel usage and the aims to phase out fossil fuel part of the fuels by 2030. Several studies have shown that replacing conventional fossil fuels with oxygenated alternatives reduces soot formation [6, 20, 21]. A rule of thumb for drop-in fuels (e.g., gasoline with 30–40% butanol) is that they should reduce engine-out soot emissions by around 50%. However, only a few combinations of renewable fuels have been investigated [57, 58]. The energy content of alternative fuels is typically lower than that of fossil fuels and their latent heats are higher, both of which necessitate longer fuel injection periods. This may influence the combustion process and soot formation [6, 20]. Soot formation when using these fuels may also be affected by fuel properties that influence spray atomization, such as vaporization behaviour, the adiabatic flame temperature, viscosity, and surface tension. In addition, the inclusion of renewable fuels may affect spray properties such as droplet size and the liquid penetration rate [6]. However, the effects of these properties on soot formation are unclear. A better knowledge of their effects (or lack thereof) is therefore needed to develop soot-reduction strategies tailored to specific renewable fuels. In addition, the potential benefits of renewable and drop-in fuels on the emissions of sub-23 nm particulates remain to be determined.

Alternative fuels offer a potential pathway to reducing vehicular well-to-wheel CO<sub>2</sub> emissions [59] and particulate emissions [21, 6, 60]. Many substances have already been identified as renewable fuels or fuel components, such as ethanol, which is the classic biofuel. In addition to alcohols, research on oxygenated fuels has shown that esters and ethers could be useful renewable fuel components for GDI applications [22, 6, 61] along with dimethyl carbonate [62]. Moreover, it has been shown that the use of alternative fuel blends can reduce engine-out emissions of CO and HC [63]. Oxygenated fuels typically have higher vapor pressures than gasoline as well as significantly higher  $\Delta H_{\text{vap}}$  (kJ/kg stoichiometric mixture) values and significantly lower LHVs. All of these features are likely to affect the quantity of fuel injected into the cylinder, as well as the spray evaporation once the fuel has been injected. Therefore, determining the effect of a given alternative fuel on PN emissions is challenging, especially since their effects may also depend on the design of the combustion system and the engine operating point. However, all oxygenates contain C-O bonds, which promote the oxidation of soot precursors and should thus tend to reduce PN emissions.



### 2.4.7 Role of alternative fuels at cold starts

The cold-start problem in internal combustion engines has received a lot of attention, especially in engines using fuel mixtures containing alcohols such as ethanol and methanol. Although ethanol and methanol are renewable and have been put forward as fuels of the future, an internal combustion engine running on them would typically have cold-start issues due to their low cetane number, high latent heat, and high ignition temperature leading to higher fuel consumption [6]. Engines produce substantial hazardous emissions during the warm-up process following a cold start – for example, the majority of hydrocarbon emissions from an engine during a typical driving cycle are thought to occur during the cold-start/warm-up phase because of incomplete combustion while the engine is cold. Replacing gasoline with alternative fuels such as ethanol and methanol could exacerbate this problem. Furthermore, high alcohol concentrations are known to hinder upper engine lubrication and erode engine components such as cylinder walls and crank bearings, resulting in premature engine failure. In some cases, it may be necessary to employ a lubricant other than those traditionally used in gasoline direct injection engines [64]. Such issues may obstruct the use of fuel blends with high contents of ethanol or methanol.



# 3 Experimental Setup and Methods

## 3.1 Engine

The experimental investigations were conducted on a single cylinder, naturally aspirated gasoline direct injection (GDI) research engine whose specifications are listed in Table 3.1. The engine was equipped with a four-valve cylinder head with intake ports generating a moderate level of tumbling gas motion. The fuel injector was centrally mounted on the spray-guided cylinder head and the fuel was conditioned using an AVL733S unit.

Table 3.1: Engine Specifications

	<b>Single-cylinder engine</b>	
<b>Cylinder volume</b>	500	cc
<b>Bore</b>	82	mm
<b>Stroke</b>	90	mm
<b>Engine head</b>	Four valve SGDI	
<b>Spark plug</b>	Single electrode	
<b>Injector for DI</b>	Six-hole solenoid injector	
<b>Injection pressure for DI</b>	200 - 350	bar
<b>Injector for PFI</b>	Conical Spray type injector	
<b>Injection pressure for PFI</b>	3.5	bar
<b>Intake air temperature</b>	35	°C
<b>Coolant temperature</b>	80	°C
<b>Inlet Valve Opening</b>	356	CADaTDC*
<b>Inlet Valve Closing</b>	578	CADaTDC*
<b>Exhaust valve opening</b>	145	CADaTDC*
<b>Exhaust valve closing</b>	357	CADaTDC*
<b>Piston</b>	Flat piston with a 2 mm deep in-bowl starting 10 mm from edge Slight cuts for valves	

\*TDC implies TDC combustion

Two different engine heads were used to investigate the formation and sources of soot in a GDI engine. A single cylinder engine with a metal head and a dual injection setup was initially used to study soot formation at high load by adjusting the homogeneity of the fuel-air mixture. This head was subsequently replaced with a custom-made metal one with endoscope access to visualize in-cylinder combustion and locate soot sources in the combustion chamber.

### 3.1.1 Naturally aspirated metal engine and operating conditions

The naturally aspirated engine with a metal head was also equipped with a PFI injector to enable dual injection operation. Fuel could thus be injected into the cylinder via a) a six-hole solenoid injector mounted centrally in the cylinder head and/or b) a port fuel injector mounted 50 cm upstream of the intake port in the inlet manifold, as shown in Figure 3.1. The two injection systems were used both simultaneously and separately in the first part of the thesis. The specifications of the injectors are listed in Table 3.1.

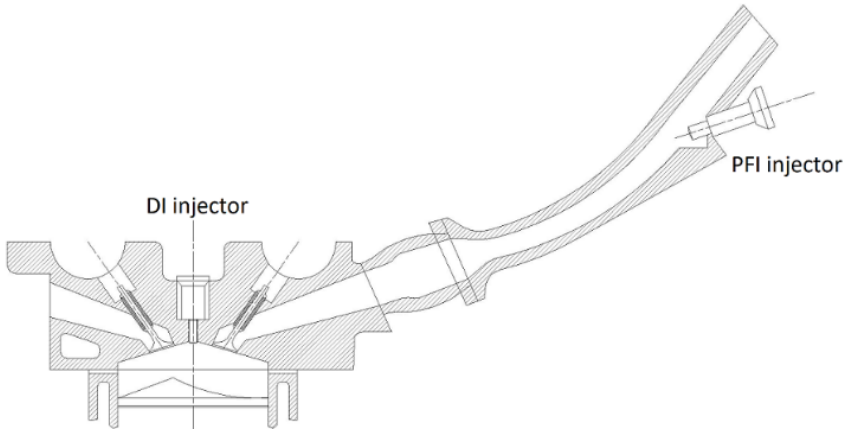


Figure 3.1: *Schematic depiction of the dual injector setup showing the centrally mounted DI injector and a PFI injector mounted 500 mm upstream in a custom manifold.*

The PFI injector was placed relatively far from the cylinder head so fuel delivered via this injector can be assumed to be well-mixed with air when it reaches the combustion chamber. The amount of fuel injected into the cylinder was quantified in units of mass. In cases where both injectors were used, the total fuel mass injected into the cylinder at a given load was kept constant. All tests were run under stoichiometric conditions with Maximum Break Torque (MBT) combustion phasing, meaning that 50% Mass Fraction Burnt (MFB50) occurred at 8 CADaTDC.

The first part of the work presented in this thesis consists of data obtained using a standard metal cylinder head. Although the experimental engine was a laboratory-scale single cylinder engine, the objective of this thesis was to study PN emissions under operating conditions representing those arising while driving a passenger car in real life. To investigate the capabilities of different PN control mechanisms, it was first necessary to establish a baseline. The baseline data were all obtained using the metal engine head and validated using exhaust PN measurements. Two main investigations were performed using the metal head. One focused on characterizing PN emissions at high load while

using a dual injection scheme to enhance air-fuel mixing. The second examined the effects of oxygenated fuels on PN emissions. In both cases the naturally aspirated experimental engine was operated under full load, producing 9 bar IMEP.

## Operating conditions for dual injection experiments

The test GDI engine was modified to enable the use of both direct injection and port fuel injection, either individually or in combination. Combining a low-pressure port fuel injector with a high-pressure DI injector created new possibilities for injecting fuel into the engine similar to those enabled by the Audi 2.0-liter EA888 Gen3 engine of 2014 and some designs by Toyota. Combining DI with PFI could reduce diffusion flame formation and thereby reduce the potential number of soot formation sites. This modified engine was used to investigate the effect of varying the fuel injection pressure and start of injection (SOI) timing on PN emissions to identify optimal parameter settings for subsequent studies. The fuel injection pressure for DI was set to 200 bar because lower pressures gave higher PN emissions at all operating points.

Particle number emissions were measured in raw exhaust samples and in samples passed through a volatile particle remover consisting of a thermodenuder and a catalytic stripper to isolate solid particles. This approach provided deeper insights into PN formation within the engine than would have been possible by measuring only raw PN emissions. Design of experiments was used to generate a factorial design in which PN measurements were acquired while operating the engine with injection mass splits between 0 and 100% PFI over a range of speeds and loads representing a high load and low speed engine operating region that produces relatively high PN emissions (see Figure 3.2). This made it possible to minimize the number of testing points while still establishing a reliable basis for analysis with at least 90% significance. The results obtained from the factorial design were modelled to a response surface using MODDE, a DOE program for statistical analysis.

The injection timings for the PFI and DI injectors were optimized individually with respect to PN emissions by measuring PN emissions over a start of injection (SOI) timing sweep at a reference load point of 5 bar MEP with an engine speed of 1500 rpm. This sweep indicated that the optimal SOI timings for DI and PFI were -270 CAD and -90 CAD before combustion top dead center (TDC), respectively.

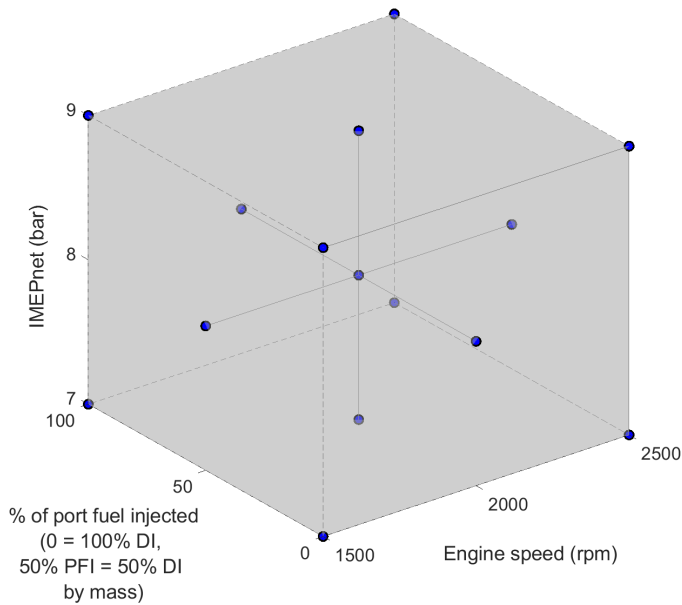


Figure 3.2: Measurement matrix showing the central composite face experimental design. The test points are shown in blue.

## Operating conditions for alternative fuel study

The experimental matrix was also used as a reference when testing the effects of alternative fuel blends on particulate emissions. Three fuels were used in these experiments, with the first being non-oxygenated gasoline. The other two fuels were blends consisting of non-oxygenated gasoline as a base fuel together with oxygenates added to the maximum level permitted by the EN 228 standard. The first blend contained 10% ethanol (EtOH) and the second contained 22% (v/v) ETBE. These blends are referred to as g+EtOH and g+ETBE, respectively. The specifications of these fuels are shown in Table 3.2. SOI optimization was achieved by performing an SOI sweep for each fuel at the reference operating point to identify the range of SOI values that minimized PN emissions. These sweeps indicated that there was no common optimal SOI timing for all fuels that would facilitate comparative analysis (see paper II for more information). The mass of fuel injected was adjusted to ensure that the total injected energy content was the same in all experiments at the same load point; consequently, the injection duration was higher for the oxygenated blends than for neat gasoline.

Table 3.2: Properties of the tested fuels\*

Property	Non-oxygenated gasoline <sup>+</sup>	g+EtOH	g+ETBE
Oxygenate content	No oxygenates	10 vol-% EtOH	22 vol-% ETBE
Oxygen (wt-%)	<0,05	3,14	3,65
RON	96,1	96,6	97,2
MON	86	86,1	86,8
Vapor pressure (kPa)	68,9	72,3	65,9
Sulphur (mg/kg)	10	8	6
Aromatics (vol-%)	30,5	29,2	26,3
Olefins (vol-%)	14,4	11,4	9,1
Density (kg/m <sup>3</sup> )	737,3	745,1	742,4
Carbon (wt-%)	86,49	83,51	82,95
Hydrogen (wt-%)	13,49	13,37	13,41
Lower Heating Value (MJ/kg)	43,202	41,722	41,442
Stoichiometric (A/F) ratio	14.58	14.65	14.68

\* Values obtained from suppliers or the literature

<sup>+</sup> Reference fuel

All tests were performed at a constant engine speed of 2000 rpm with a load of 4.5 or 9 bar IMEP (see Table 3.3).

Table 3.3: Experimental test matrix and corresponding engine parameters

Test point	Fuel blend	Speed/IMEP <sub>net</sub>	PN sample
<b>1</b>	Gasoline g+ EtOH g+ ETBE	2000 rpm/ <b>4.5</b> bar	Raw, TD
<b>2</b>	Gasoline g+ EtOH g+ ETBE	2000 rpm/ <b>9</b> bar	Raw, TD

Because the aim was to isolate the effects of fuel composition on PN emissions and minimize variation in mixture formation, the engine was not fitted with a tumble flap. Additionally, the engine speed was kept constant throughout. Experiments were performed at load points of 4.5 and 9 bar IMEP. The 9 bar IMEP load point, which is close to wide-open throttle conditions for the studied engine, was included because higher loads lead to higher exhaust gas temperatures, which have important effects on engine aftertreatment systems. The maximum IMEP at full load was limited by knock and the maximum cylinder pressure, making it impossible to conduct experiments at load points above 9

bar IMEP.

### 3.1.2 Metal cylinder head with optical access

A custom-made metal cylinder head providing optical access to the combustion chamber via an integrated endoscope was used in all subsequent experiments to gather visual information on the combustion process and deepen the understanding of PN formation. Importantly, the endoscope head behaves like a metal engine head, allowing the engine to withstand operation at higher loads than can be tolerated in conventional optical engines. This is important because the “high” load point of 9 bar IMEP examined in these studies is actually rather moderate by the standards of modern GDI engines, so any restriction that required further reductions in load would reduce the value of the gathered data. Aside from the inclusion of the endoscope and a slight reduction in the cylinder volume from 500 to 495 cc, the engine’s specifications were unchanged by the modification (see Table 3.1 for details). Fuel was injected using the same centrally mounted direct injector as in the previously described experiments. Corrections were made to account for the difference in cylinder volume where necessary during the analysis.

Optical access to the combustion chamber was provided for an endoscope and a plasma optic light guide, the latter of which was used to provide illumination for images before the start of combustion so that the mechanism of fuel transport into the combustion chamber could be visualized. However, at an injection pressure of 300 bar, the fuel spray images provided little useful information. Most of the time, the illumination was only used to obtain background images for image analysis. The setup is shown in Figure 3.3.

The viewing angle of the endoscope was 12 degrees from the horizontal piston top. Special attention was paid to the stiffness of the mounts holding the high-speed camera because vibrations from the engine during operation could damage the cameras and reduce image stability. The camera was therefore mounted on an independent table to minimize blur and was situated in-line of sight with endoscope as shown in Figure 3.5. The trigger signal to the camera was synchronized with the spark timing to ensure that high-speed video recording was initiated by the start of combustion. Figure 3.4 shows an inside view of the cylinder captured through the endoscope in the stationary engine with illumination. An Ametec Vision Research Phantom Miro M310 high-speed video camera with a Carl Zeiss 85 mm f/2 lens was used for imaging. The rate of image acquisition was controlled using Phantom Camera Control (PCC) and was set to a framerate of 12000 frames/s, corresponding to two images with a resolution of 512x480 per CAD with an exposure time of 50  $\mu$ s.

### 3.1.3 Pre-conditioning of the engine and the measurement system for investigation of history effects

In most of these experiments, the fuel injector was centrally mounted on the spray-guided cylinder head and the PFI and its custom manifold were dismantled. A LabVIEW cRIO real-time hardware/software-controller was used to establish cycle-resolved control



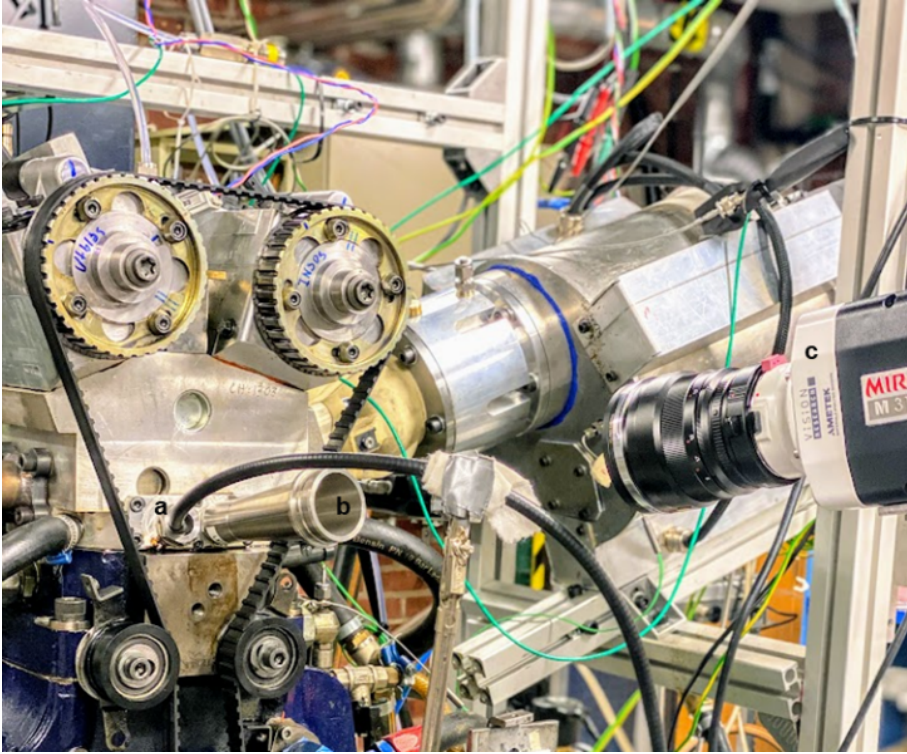


Figure 3.3: Setup of optical access to combustion chamber showing assembly of (a) light source, (b) endoscope and (c) high-speed camera

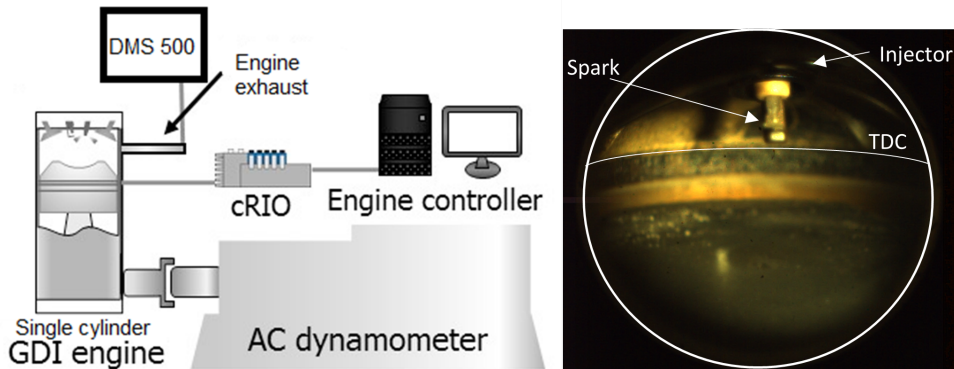


Figure 3.4: Schematic of experimental setup showing cRIO and engine controller along with sampling of raw exhaust along with endoscope view into the cylinder

over injection timing and fuel injection parameters such as the SOI timing and duration as well as the number of injections. An AC dynamometer was coupled to the engine

to control the engine speed and torque. Fast sampling of engine data including the in-cylinder pressure as well as spark and injection signals were collected using the AVL Indicom software. The in-cylinder pressure was measured with a 0.5 CAD resolution using a Kistler pressure transducer that was installed in the cylinder. A schematic depiction of the engine system is presented in Figure 3.4.

To obtain stable and reproducible particulate data, the engine needed to have been turning over with the particulate measurement systems running for at least a minute. This process is henceforth referred to as pre-conditioning. Pre-conditioning was preceded by the engine being at rest, followed by a few cycles of engine motoring and then some combustion cycles at 9 bar NMEP. During the pre-conditioning process, the coolant water temperature was constant but the piston temperature increased, which affected the subsequent PN measurements.

Other factors could also impact PN formation during pre-conditioning, such as build-up of hydrocarbons on the internal surfaces of the exhaust pipes and sampling system, which could cause long-term variance in PN formation [65]. In fact, these storage-release processes can cause variations in measured PN concentrations that are several orders of magnitude larger than engine-out particulate emissions. Analyses conducted in accordance with the Particle Measurement Programme (PMP) [66] showed that pre-conditioning had no obvious effect on PM but did significantly affect PN. In accordance with this finding, it has been shown that pre-conditioning diesel engines at higher load points leads to higher PN emissions in subsequent tests. This was tentatively attributed to increased inertial deposition at higher loads, although this explanation is inconsistent with the findings of Rojas [67] and Yokoi et al. [68], who showed that periods of idling followed by higher power operation produced higher PN emissions in a diesel engine. This could be due to lowered piston temperature. They also demonstrated increased levels of re-entrainment during high speed, high load operation. Under these conditions, PM release occurred because of high exhaust temperatures.

The volatiles that are released at high temperatures briefly increase the volatile saturation ratio, causing an increase in the abundance of nucleation mode particles due to gas-to-particle transformations. To quantify the variation in PN measurements obtained using the DMS500 system, ten repeat measurements were taken while conditioning the engine for 1000 cycles at the baseline operating point (meaning that the engine was operated with a fixed injection timing of -310 CAD to achieve a load of 9 bar NMEP at 2000 rpm). This SOI timing consistently minimized PN emissions from the studied engine (see 2.6) and was therefore used as a baseline, as mentioned previously. Under these conditions, 50% mass fraction burned was reached at 8 ATDC (CA50 @ 8 ATDC). Between tests, the engine was turned off and allowed to stand still for at least 12 hours. The results of these experiments are shown in Figure 3.5. The minimum and maximum PN measurements recorded over these 10 test days differed by only 24%. The number of motoring cycles preceding the combustion cycles had no significant effect on PN levels at the end of the pre-conditioning period.

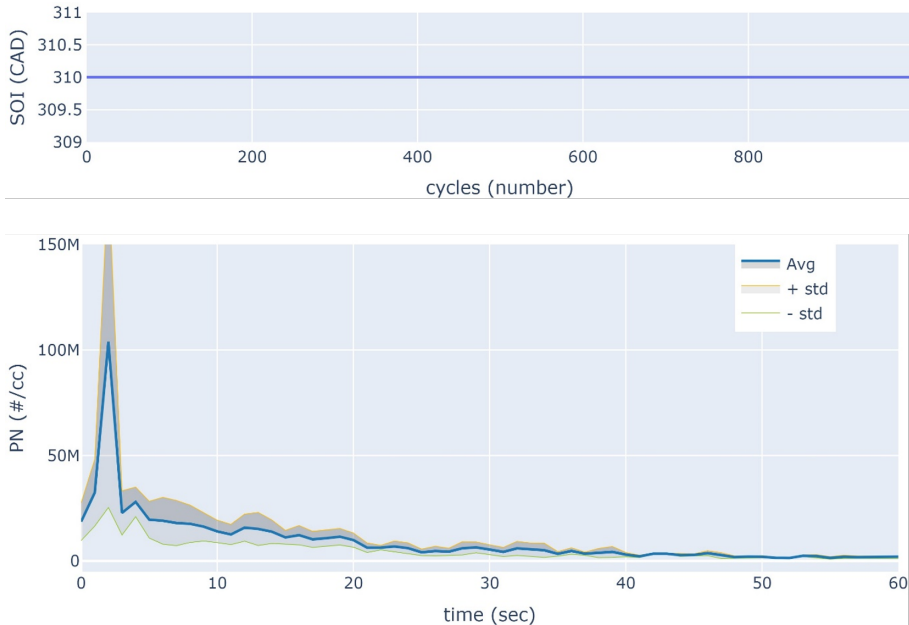


Figure 3.5: *PN emissions from 10 repeats of pre-conditioning for a baseline load of 9 bar NMEP and SOI of -310 CAD at an engine speed of 2000 rpm*

After successful convergence of PN measurements over 1000 cycles (roughly 50 s), the engine had reached a steady state. The pre-conditioning process thus successfully established stable conditions, meaning that subsequent combustion cycles within the test sequences were unaffected by factors such as temperature effects from preceding cycles. All of the SOI variation sequences that were examined in this study were preceded by 60 seconds of pre-conditioning cycles to obtain stable and reproducible PN measurements.

### 3.1.4 Procedure for visualizing soot sources during load transients

Transient operation presents a unique challenge for any laboratory engine because most dynamometers are specifically designed for stationary load point operation. Load points are usually defined based on the engine's speed and load. The engine speed affects mixing and thus influences combustion, soot formation, and PN emissions. However, it generally does not affect PN emissions as strongly as the load. Consequently, only load transients were examined in this work. The analysis of transients focused mainly on spray-wall interactions because they were consistently found to be the dominant soot source.

Figure 3.4 shows the novel cRIO module that was developed to provide precise cycle-to-cycle control over engine parameters and implement pre-programmed engine operation sequences such as load transients. The ability to deterministically adjust engine parameters on a cycle-to-cycle basis also made it possible to study previously overlooked factors

affecting PN emissions such as the history effect, which was discovered during the studies included in this thesis. This module makes it possible to increase the engine's load in a controlled manner over successive cycles, allowing a load transient to be generated within 2 seconds, which is comparable to the situation in a passenger vehicle starting on full load immediately after start-up.

The main purpose of these experiments was to investigate PN formation during load transient conditions. To this end, engine operating parameters associated with PN emissions such as the start of injection (SOI), air-fuel ratio ( $\lambda$ ), and the coolant temperature were varied systematically over the load transient sequence shown in Figure 3.6. The sequence began with engine motoring for 30 seconds, followed by firing for another 30 seconds at 4 bar NMEP and an engine speed of 2000 rpm. This was immediately followed by a rapid increase in load to 12 bar over 2 seconds, corresponding to 33 cycles. During the load transient, the throttle, injection, and ignition parameters were dynamically varied. Finally, the engine was allowed to run for about 3 minutes to stabilize at the higher load. During the evolution of experimental campaign with the engine, it was observed that measured PN emissions can be highly variable during fast events. Therefore, the durations of the different parts of the transient sequence were chosen to minimize this variance. The engine was motored for 500 cycles to clear residual soot build-up from the previous run. It was then fired at 4 bar for another 500 cycles to pre-condition the engine and stabilize its PN emissions. Two seconds was found to be the minimum time needed for data sampling during a transient because of the sampling rate of the equipment and the time needed for dilution.

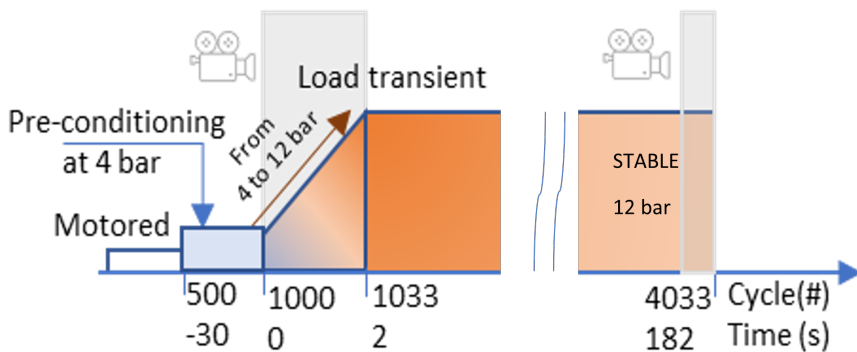


Figure 3.6: Load transient sequences and load variation as functions of the cycle number and time at an engine speed of 2000 rpm. Cycles that were filmed are indicated by pictures of cameras and a grey background

Precise cycle-to-cycle control of the air-fuel (A/F) ratio is essential during an experimentally induced load transient. To enable this, the analogue throttle motion during

the transient was varied linearly between predefined initial and final values. This caused a non-linear increase in the trapped mass in the cylinder. The corresponding fuel mass curves were calculated to match this increase. Figure 3.7 shows the evolution of the throttle opening (in terms of the intake pressure), the load (in terms of NMEP), and cylinder pressure during a stoichiometric load transient from 4 to 12 bar NMEP over 33 cycles at 2000 rpm and 15 °C. The throttle opening, injection duration (DOI), spark, and timing were automatically adjusted throughout the load transient in all test cases to maintain stoichiometric operation with a CA50 of around 7-8 CADaTDC.

Several factors can affect soot formation during load transients both positively and negatively. One such factor is impingement of fuel on the piston. The impact of this factor was minimized by fixing the injection timing during the transients so that the distance between the injector and the piston at the end of injection increased as the transient progressed, reducing the risk of piston impingement by fuel injected towards the end of injection. Another factor is that higher loads lead to higher combustion temperatures, and thus higher rates of fuel vaporization. A third factor is that, stationary operation at high load leads to higher piston top temperatures [13], which reduces wall film build-up. However, during a transient there is insufficient time for the temperature to stabilize to reflect the load.

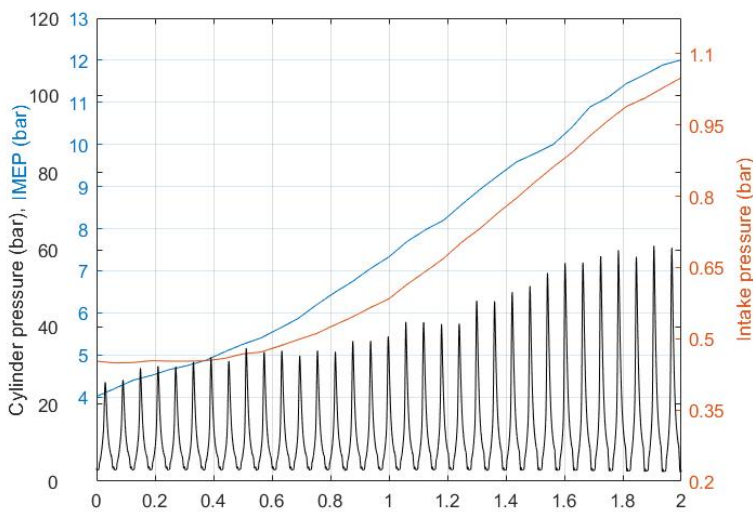


Figure 3.7: *Evolution of the cylinder pressure, intake pressure, and resulting NMEP during a load transient at 2000 rpm with a coolant temperature of 15 °C.*

Table 3.4 lists the experiments conducted to investigate the influence of selected parameters on PN formation at different coolant and oil temperatures. In this work, the phrase “coolant temperatures” refers to both engine coolant and oil temperatures. Different

coolant temperatures lead to different surface temperatures in the combustion chamber, which influences the mechanisms of PN formation. The first set of experiments was done to study the effect of coolant temperature, with all other parameters held at their optimum values. Supplementary experiments were then performed to investigate the effect of varying the air-fuel ratio under the same conditions. The second set of experiments used a split injection strategy, which was expected to reduce liquid film formation by reducing liquid fuel penetration and possibly also enhancing tumble motion that promotes mixing. The third set used a delayed start of injection (SOI) timing of -270 CAD. Delaying injection was found to reduce PN emissions under warmup conditions at lower loads [see results chapter]. Three replicates were performed for each set.

Table 3.4: Operating conditions for load transient experiments

Set	Set name	Lambda	Inj. timing (CADbTDC)	Coolant & Oil temp. (C)	PN data	Images
1	Stoich -310 (Baseline)	1.0	-310	15,45,60,90	Yes	Yes
-	Rich, Lean	0.9,1.1	-310	15,45,60,90	Yes	No
2	Split injection	1.0	-310 and -230 (50% mass split)	15,45,60,90	Yes	Yes
3	Later Injection	1.0	-270	15,45,60,90	Yes	Yes

\* The fuel profile from set 1 was adjusted to establish global lambdas of 0.9 and 1.1 for rich and lean transients

## 3.2 Measurement Setup

### 3.2.1 DMS500

A Cambustion DMS500 MkII fast particle analyzer was used to monitor the particle distribution and number of particles emitted from the engine by measuring the electrical mobility of each particle. The instrument works by sampling exhaust and passing the exhaust gas sample through a corona charger that gives each incoming particle a positive charge proportional to its surface area. The charged particles then enter a classifier column (Figure 3.8) where they are separated according to their charge and aerodynamic drag. An amplifier converts the resulting currents into data on particle numbers and sizes. The DMS500 is equipped with a build-in dilution capability which consists of a primary and a secondary diluter. The secondary diluter was kept at a factor of 1 for strong signal strength. The dilution factor was kept constant during the measurements because particle size measurements depend strongly on dilution. The sample in the primary diluter was heated to its maximum of 150 °C. To avoid condensation in the sampling line, it was heated to 150 °C all the way from engine to the DMS using an external heating agent. A uniform temperature was maintained over the sample line to avoid losses due to temperature gradients.

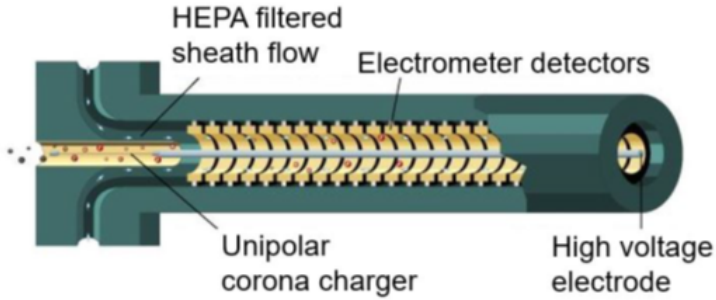


Figure 3.8: *Key components of the DMS500 particle size measurement system [Cambustion 16]*

The DMS500 was cleaned daily to eliminate measurement errors due to accumulation. The flow through the thermodenuder was maintained at the recommended value of 15 lpm. All measurements were conducted under stable steady state operating conditions with a Coefficient of Variance (CoV) in IMEP  $< 1.5\%$  where possible. However, when using 100% PFI at high load, it was impossible to reduce the CoV in IMEP to much less than 3%.

The experimental data were analyzed using a Partial Least Squares (PLS) regression model, which required scalar input data. To generate suitable scalars from the raw DMS500 data, we summed the average counts for each particle size class considered in this work over the measurement duration. This approach is consistent with the method for characterizing particulates specified in the PMP standard [45]. The DMS500 has a measurement threshold of  $10^3$  particles per unit flow ( $dN/d\log D_p/cc$ ); the iso-lines indicating 0 PN in some of the plots from the analysis correspond to exhaust samples whose particulate content was below this threshold value.

The PN distributions from the DMS500 were recorded for at least three minutes under stable engine operating conditions with a frequency of 5 Hz and averaged to obtain stable and reproducible data.

### 3.2.2 Thermodenuder

Particulates were measured both with and without a VPR using two switchable valves from the engine exhaust manifold to the DMS500, as shown in Figure 3.9. A Dekati thermodenuder (TD) acting as a VPR and a monolithic catalytic stripper (CS) were used to remove volatiles and ensure that only solid particles were measured. Both the TD and CS were heated to  $350\text{ }^\circ\text{C}$  and the exhaust was sampled approximately 15 cm downstream of the exhaust port. Unlike the PMP standard, which uses a dilution-based VPR, the method applied in this work uses no external dilution because it was found that the signal strength was reduced excessively when dilution was applied.

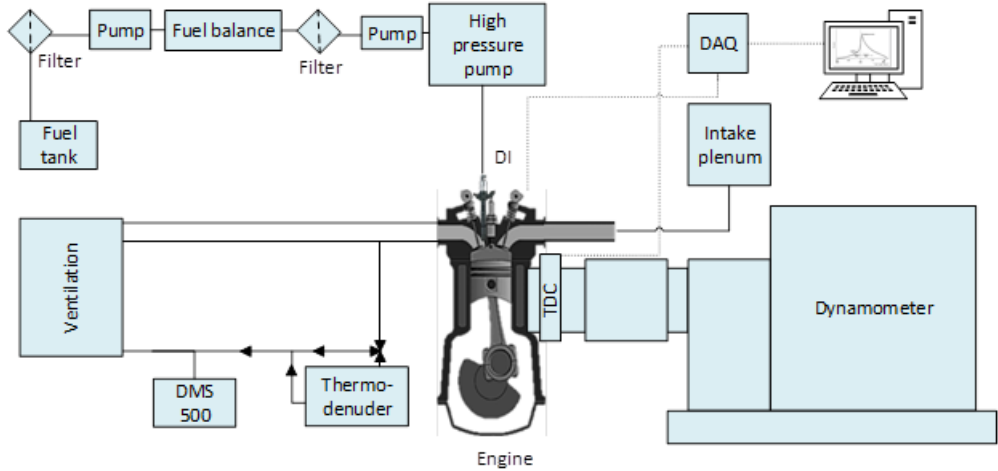


Figure 3.9: *Measurement apparatus used to show switching enabled to sample engine exhaust with and without thermo-denuder*

A thermo-denuder removes volatiles via a two-stage process: first the incoming exhaust is heated to evaporate volatile compounds, then the dry exhaust is passed through an adsorbing carbon cartridge surrounded by cooling water, as shown in Figure 3.10. At the beginning of each test campaign, a fresh carbon cartridge was installed to ensure adequate adsorption of volatile compounds [69]. Note that particulate numbers in raw exhaust are referred to as PN while those measured after passage through a TD are referred to as solid PN.

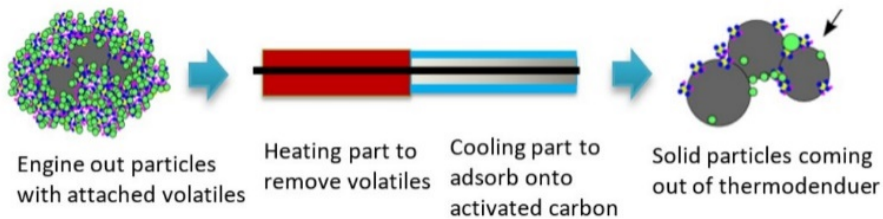


Figure 3.10: *Working principle of a thermo-denuder showing the removal of volatile organic compounds from engine out particles*

The penetration efficiency, which is influenced by the residence time and temperature, can be used to quantify adsorption processes in a TD. By maintaining the Dekati-recommended flow rate, losses from diffusion in the TD were reduced to a minimum. The system's penetration efficiency was discovered to be respectable, with minimal losses in comparison to the quantity of exhaust particles. These findings show that the majority of



the PN emissions measured while utilizing the TD were made up of solids [14].

### 3.2.3 Methodology for image analysis

The images obtained by endoscope visualization of combustion process in the cylinder were processed to obtain quantitative data and establish correlations with the PN concentrations measured in the engine exhaust. Only the combustion part of the cycle was visualized and analyzed at each load point. At 12000 frames per second and an engine speed of 2000 rpm, this meant that only about 120-130 frames were analyzed per cycle, depending on the memory gate. Each frame represented half a CAD at this sampling rate. Figure 3.11 shows the conversion of a raw true-color image into a binarized image after selecting the red color channel. Binarization is usually done by applying a suitable threshold, preferably one that effectively differentiates the yellow flame from the rest of the image. However, in some cases the yellow flame's intensity (which depends heavily on the engine load) is so high that it saturates the whole frame. In such cases, it is difficult to obtain visual information. However, such behaviour typically only persists over a few frames while the flame front travels towards the cylinder walls and covers the lens or during full load operation. In our experiments, we were primarily interested in detecting slow-burning yellow flames associated with fuel-rich zones or fuel pyrolysis due to a thick wall film. These wall films mainly occurred on the piston top because the engine had a centrally mounted injector, so at odd SOI timings the liquid spray could interact directly with the piston surface.

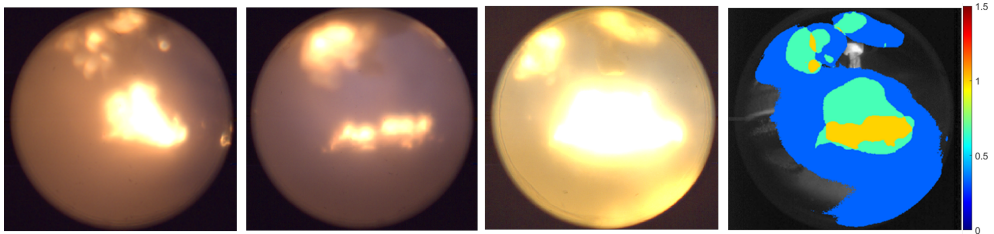


Figure 3.11: *Frequency analysis to locate soot sources based on single shot combustion images captured at 50 CAD from ignition mid-way through three load transients (at 6bar NMEP). Coolant temperature = 15 °C, SOI = -310 CAD, engine speed = 2000 rpm.*

It is straightforward to locate yellow flames in binarized images because they appear in white while the rest of the frame is black. Twenty successive combustion cycles were filmed during operation under stationary load and the resulting binarized images were analyzed to determine the relative frequency at which yellow flames occurred. This approach was subsequently applied to images acquired during transient operation; in this case it was not possible to analyze images from successive cycles, but the entire transient was repeated several times at each load point to obtain sufficient data for frequency analysis.



# 4 Summary of publications

This chapter briefly summarizes the contents of the publications arising from the research conducted to date during this PhD project. The results obtained are discussed holistically and in more detail in the following chapter (Results and Discussion).

## 4.1 Paper I

*"Particulate Emissions in a GDI with an Upstream Fuel Source"*

Paper I presents experimental studies on PN emissions from GDI engine equipped with a custom inlet manifold and a port fuel injector located 500 mm upstream. Particulate emissions were measured during stationary medium/high load operation to evaluate the effect of varying the mass split between the direct and upstream injectors. Mixing quality was improved substantially by upstream injection and could thus be controlled by altering the mass split between the injectors. Particulate measurements were performed using a thermodenuder and a catalyst to remove the majority of the volatile organic compounds (VOCs) from the raw emissions, which made it possible to determine particle numbers (PN) for both raw emissions and solid particulates only, and to evaluate the size distribution of the solid particulate emissions. Combining direct injection with upstream port fuel injection was found to reduce PN emissions by almost a factor of 10 under optimal conditions, and significant reductions were achieved even when only 10% of the fuel mass was injected upstream. At a fixed load, increasing the mass percentage of fuel injected upstream reduced PN emissions. However, the PN reduction achieved in this way was load-dependent and sensitive to engine speed. Solid PN emissions decreased almost linearly with the PFI mass percentage, independently of engine speed. This implies that upstream injection improved mixing and thus reduced rich zone formation and/or wall-wetting when compared to exclusive direct injection.

The author of this thesis constructed the apparatus used in these experiments at Chalmers Tekniska Högskola (CTH) with support from Alf Magnusson and Timothy Benham, designed and performed all experiments and data post-processing, and wrote the paper. The author also presented the paper at the SAE World Congress Experience in Detroit, Michigan 2019. The work presented in this publication was supervised by Petter Dahlander, Lucien Koopmans, Mats Laurell and Ayolt Helmantel.

## 4.2 Paper II

*"Effect of Renewable Fuel Blends on PN and SPN Emissions in a GDI Engine"*

Paper II presents a comprehensive study on the effects of renewable fuel blends on PN and SPN emissions. PN emissions were measured using a DMS500 instrument, and the same instrument was used in conjunction with a thermodenuder to measure SPN emissions. At early SOI timings, where particulate formation is dominated by diffusion flames on the piston resulting from liquid film formation, the oxygenated blends yielded dramatically higher PN and SPN emissions than reference gasoline because of fuel effects. When applying optimized SOI timings at low load (4.5 bar IMEP), the use of oxygenated blends significantly increased emissions of solid particulates having diameters  $> 23$  nm but reduced raw PN emissions. At high load (9 bar IMEP), overall SPN emissions were significantly higher and there were no clear differences between the blends. Additionally, SPN measurements showed that soot formation and emissions of volatile organic compounds (VOC) depended strongly on blend composition. Finally, adding oxygenates (up to 22%) to gasoline did not reduce SPN emissions in the size ranges addressed by current regulations.

The comparatively low engine loads examined in this paper necessitated analysis of small particles, most of which were volatile. This posed challenges that made it necessary to conduct two separate experimental campaigns. The author of this thesis constructed the experimental setup at CTH with support from Alf Magnusson, Timothy Benham, and Jonas Sjöblom, performed all of the experiments and post-processing, and wrote the paper. The author also presented the paper at SAE PFL digital summit 2020. The work presented in this publication was supervised by Petter Dahlander, Lucien Koopmans, Ayolt Helmantel, and Anna Karvo.

## 4.3 Paper III

### *"Soot Sources in Warm-Up Conditions in a GDI Engine"*

Paper III explores the effect of individually varying the temperature of the coolant and oil in a GDI engine to determine which factor has the greater influence on PN emissions. Whereas coolant temperature strongly influenced PN with cold oil, the oil temperature had little effect on PN emissions at low coolant temperatures. These findings indicate that PN emissions depend heavily on the engine block's temperature, which is dominated by the coolant. The SOI timing also strongly affects PN formation because it influences the wall film thickness on the piston top. Under experimental warm-up conditions, injecting fuel at a later SOI reduced PN emissions. Moreover, visualization of in-cylinder events revealed that no diffusion flames were formed at late SOI timings, presumably because the use of such timings prevented or greatly reduced impingement of the liquid fuel on the piston. The integrated luminescence from combustion images correlated closely with measured PN emissions: higher integrated luminescence values resulting from pool fires on the piston top were associated with greater soot formation and thus higher PN emissions. When the coolant and oil temperatures were varied simultaneously, PN emissions were found to decline dramatically with increasing temperatures. At lower temperatures, diffusion combustion occurred on the piston due to a persistent film of liquid fuel. This film was relatively thick and persistent when the coolant and oil temperature were both 15 °C but it gradually disappeared as the temperature increased. When the temperature reached 60 °C, diffusion flames became less common, drastically reducing PN emissions.

The author of this thesis constructed the experimental single cylinder metal engine with optical access with support from Alf Magnusson, performed all of the experiments and post-processing, and wrote the paper. The author also presented the paper at SAE WCX Digital Summit 2021. The work presented in this publication was supervised by Petter Dahlander and Ayolt Helmantel.

## 4.4 Paper IV

*"History Effect on Particulate Emissions in a Gasoline Direct Injection Engine"*

Paper IV presents a comprehensive study on a previously unrecognized dynamic phenomenon affecting particulate emissions that has been named the history effect. Traditionally, experimental start of injection (SOI) sweeps have been conducted by changing the injection timing in stepwise increments. However, to better understand the influence of SOI timing on PN emissions, a novel approach based on cycle-to-cycle parameter control was applied in this study. In this approach, the engine is not motored or turned off when going from one SOI timing to the next; instead, the engine was operated continuously and combustion and SOI sweeps were performed online using a series of pre-programmed and perfectly deterministic SOI sequences. During engine operation, changes in SOI lead to changes in combustion behaviour and liquid fuel impingement, creating a new engine state that influences subsequent engine states. It was therefore found that while excellent reproducibility was achieved in experiments using different pre-programmed SOI sequences, the results obtained depended strongly on the order in which the SOI timings were set. To explain this observation, in-cylinder combustion was visualized using an endoscope connected to a high-speed camera. Two SOI timings were chosen based on piston deposit level data from stationary measurements to investigate the history effect of preceding conditions on PN emissions. The results showed that the preceding engine state strongly affects PN formation and emissions and that this "history effect" was most pronounced under impinging conditions resulting from the use of early injection timings such  $-340$  crank angle degrees (CAD). The magnitude of the history effect was also found to depend on the duration of the preceding state. These results showed for the first time that PN emissions under different engine operating conditions depend on how the engine's SOI timing was varied in the recent past.

The author of this thesis designed the tested cycle-to-cycle sequences required to quantify this history effect. The author also constructed the experimental setup for the single cylinder metal engine at CTH with the support of Alf Magnusson and performed all experiments and post-processing. The author wrote the paper for the SAE International Journal of Engines. The work presented in this publication was supervised by Petter Dahlander, Lucien Koopmans and Ayolt Helmantel. The custom Compact Rio/MATLAB hardware/software solution that enabled programming of signal sequences for dynamic cycle-to-cycle control of the engine was developed by the main supervisor.

## 4.5 Paper V

*"Visualization of soot formation in load transients during GDI engine warm-up"*

Paper V presents experimental studies on a transient sequence in which the engine load was increased from 4 bar IMEP to a maximum of 12 bar IMEP over 2 seconds at an engine speed of 2000 rpm. During the transients, the engine's PN emissions were measured and images of the combustion process inside the cylinder were captured using a cylinder-mounted endoscope and a high-speed camera to identify locations where soot formation occurred. Experiments were conducted at a range of coolant temperatures and using different injection strategies to determine how these parameters affect PN emissions. The coolant temperature was found to be the dominant factor governing PN emissions during transients. Luminescence data obtained by analysing the flame images agreed well with the measured PN emissions during transients where soot was mainly formed from wall films, but not when soot formation was mixing-dominated. Varying the air-fuel ratio had little effect on PN emissions during transients. At all coolant temperatures, PN emissions were lowest when using a split injection strategy but delaying the injection timing increased PN emissions even though the endoscope images suggested a lower frequency of diffusion flame formation. No conditions were found under which the PN emissions during transients with low coolant temperatures could be reduced to levels comparable to those seen with warm coolant.

The author of this thesis designed the transient sequence after testing multiple timescales for possible load transients at an engine speed of 2000 rpm. This involved identifying a suitable injection timing, duration, ignition, and throttle position for sustainable stoichiometric operation throughout the transient. Experiments were constructed and conducted by the author on the single cylinder metal engine setup at CTH with the support of Alf Magnusson. The author also performed post-processing of the obtained data and a literature review, and wrote the paper. The work presented in this publication was supervised by Petter Dahlander, Lucien Koopmans and Ayolt Helmantel.





# 5 Results and Discussion

This thesis is based on experimental investigations into soot formation obtained with the different load points and tested fuels including transients and compares them to stationary operating data obtained from baseline GDI engine. The experiments mainly consisted of Findings are presented for standard gasoline stationary operation first and then later compared to different mixing levels or fuel blends depending on the investigation. The potential of understanding the root causes of soot formation in reducing PN emissions in a GDI engine is systematically presented through these findings in this thesis.

Firstly, mixing has a key role in keeping the charge mixture as homogeneous as possible which helps in improving the combustion and thus reducing PN (Paper I). Secondly, the presence of oxygenates does not always guarantee reduction in soot due to oxidation (Paper II). Thirdly, the spray wall interaction is by far the most dominant phenomena which is directly proportional to engine coolant temperature and in turn, correlated very well with the PN emissions in the exhaust (Paper III). Fourth, the effect of preceding engine state on current state PN emissions is quantified through wall wetting (Paper IV). Finally, increase in PN during a load transient is mainly due to wall wetting rather than the enriching of the mixture (Paper V). Further details are provided in the cited and attached publications.

## 5.1 Particulate emissions and measurements

The first half of the PhD project focused on investigating PN control strategies concerning engine technology and alternative fuels. PN contains VOCs which are further removed by using thermodenuder after engine exhaust for SPN measurements.

### 5.1.1 Investigation of PN in GDI with an upstream injector

Following literature studies on PN emissions from gasoline engines, it was understood that compared to PFI systems, DI fuel injection systems are more likely to produce less homogeneous fuel-air mixtures at ignition because they yield shorter mixing times and may cause fuel impingement on the combustion chamber and cylinder walls, the piston, or the valves. Particulate formation in gasoline engines usually results from inadequate air-fuel mixing [3]. With the aim to improve combustion quality, the first experimental campaign was focused on increasing mixture homogeneity, which is essential for minimizing particulate emissions.

Reduction in PN emissions from the metal engine was possible by combining PFI and DI systems and merging the benefits of both systems. However, the engine's operating parameters significantly affect the fundamental particle formation mechanisms active in the cylinder. A qualitative understanding of this influence could reveal parameters that could be tuned to minimize PN emissions without requiring expensive new components

by increasing mixture homogeneity to reduce wall-wetting and the formation of fuel-rich zones. These experiments therefore examine the relationship between charge homogeneity and PN emissions in a single cylinder gasoline engine. Specific attention was paid to PN measurements from the GDI engine with and without a volatile particle remover (VPR), thermodenuder in this case and compare results with a catalytic stripper. Measurements were conducted according to an experimental design that focuses on high loads (which generate high PN emissions) and a range of engine operating speeds, shown in Figure 3.2. Exhaust was sampled from the engine, through a thermodenuder acting as a VPR and a catalytic stripper sequentially.

The split of the fuel mass injected by DI and PFI will influence combustion and particulate formation. The mass from the DI injector will decrease as the PFI contribution increases, reducing its injection duration. This will reduce piston wetting and increase the mixing time, both of which are known to reduce soot formation in DISI engines [10]. The upstream port injector is a well-mixed fuel source because the fuel it injects has significantly longer to mix with the incoming air than directly injected fuel, leading to lower PN emissions. The measurements presented here cannot distinguish between the effects of the individual injection types but can show their combined effect. This is illustrated in Figure 5.1 which shows that increasing the PFI contribution reduces and ultimately almost eliminates PN emissions under the tested operating conditions.

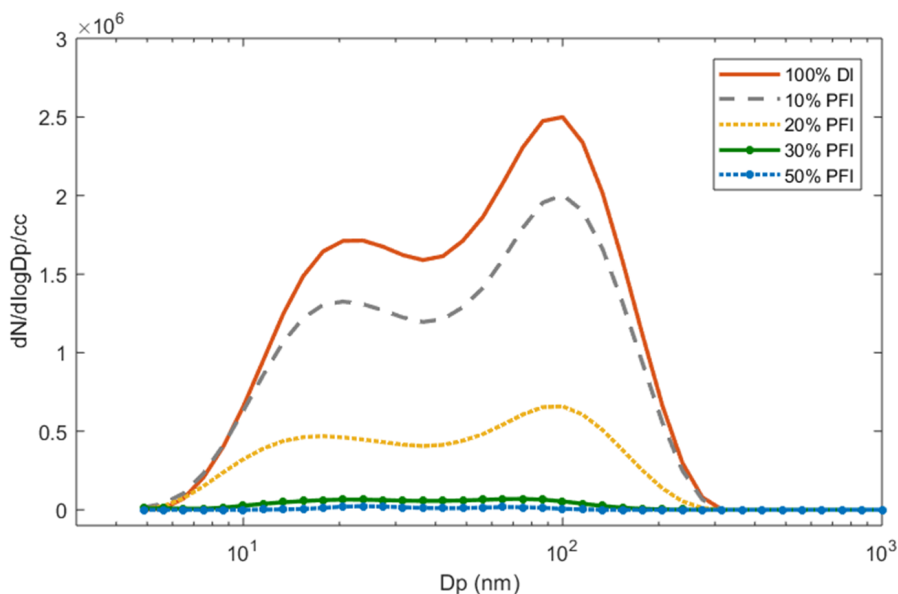


Figure 5.1: *PN in raw exhaust at 7 bar IMEP and 1500 rpm. PN emissions are highest when using DI exclusively and fall as the PFI contribution increases. [14]*

Figure 5.1 shows the effect of varying the mass split of the injected fuel on PN measurements in the raw exhaust of the engine when operating at a load of 7 bar IMEP and 1500 rpm. The plot suggests that the reduction in PN emissions upon increasing the PFI contribution was non-linear. Because increasing the PFI contribution reduces the mass of fuel injected by DI, the injection duration for the DI injector falls, significantly reducing piston wetting [10]. However, the benefit of additional reductions in the DI duration appears to decline asymptotically as the PFI contribution increases; at the studied load point and speed, the PN reductions observed at PFI contributions of 30% and 50% were roughly equal.

The sub-23 solid size particles from total PN particle counts shown in Figure 5.2 indicate that solid particles comprise a negligible proportion of total sub-23 PN emissions for PFI contributions of 10% and above. Some small volatile particles emitted under these conditions may originate from oil penetrating into the cylinder from the engine crank while the piston is in motion. However, such particles typically have diameters of 30-40 nm [70], suggesting that sub-23 particles are predominantly VOCs. Moreover, nucleation mode particles are believed to be mostly volatiles and/or semi-volatiles, which are formed largely as an artifact of the measurement systems. For instance, they are formed during the dilution of exhaust gases with air in sample lines, which is required by commercial size measurement instruments [71].

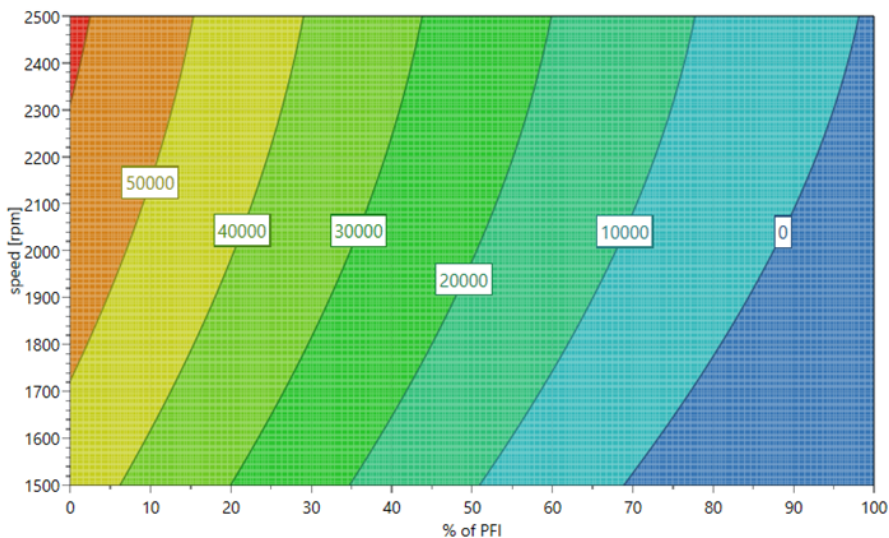


Figure 5.2: Solid PN ( $\#/cc$ ) with diameters below 23 nm in exhaust samples passed through a thermodenuder for PFI contributions between 0 and 100%. Results obtained at an engine load of 7 bar IMEP and engine speeds between 1500 and 2500 rpm. [14]

Reducing the mass of fuel injected by DI reduces PN emissions by reducing wall wetting and improving mixing quality. However, the fuel mass split was not the only factor affecting PN in raw exhaust. This suggests that VOC emissions depend strongly on engine speed and load in addition to fuel mass split, which is reflected in PN. VOCs are generally removed from engine exhaust using a warm catalyst. However, it is not very effective when the catalyst is below its activation temperature, as occurs during cold starts. In hybrids, this can also occur if the time between stop and start is too long. Under such conditions, VOCs can slip through the after-treatment system.

### 5.1.2 PN and oxygenated fuel blends

The use of gasoline-ethanol blends in gasoline engines can cause beneficial charge cooling effects that reduce CO and NO<sub>x</sub> emissions [38]. These effects can also increase net soot formation in gasoline direct injection (GDI) engines. However, studies on soot formation in GDI engines using gasoline blends with ethanol contents of 20%, 50%, and 85% revealed that increasing the fuel's ethanol content reduced both PN emissions and the size of the emitted particles [17]. These results are consistent with those of Khosousi et al. [18] and others [19]. Similarly, Zhang et al. [20] found that oxygenate addition, in general in GDI engines at moderate loads, hinders the formation of soot precursors, which can ultimately reduce PN. Similar reductions in CO, CO<sub>2</sub> and NO<sub>x</sub> emissions are observed with blends containing ETBE [21].

Some studies have shown that the presence of oxygenates in fuel can increase particulate emissions [38, 65, 72, 73, 74] while others have shown the opposite effect [6]. Consequently, the next experimental campaign identifies the conditions under which the presence of oxygenates in fuel is beneficial to reducing soot formation, and to differentiate between effects on the emissions of volatiles and solids. There are few published studies on particulate emissions from gasoline engines using gasoline blended with ETBE [74, 5]. Therefore, experimentally investigating particulate number (PN) emissions from the metal engine using fuel blends containing 10% (v/v) EtOH or 22% (v/v) ETBE paved way for understanding the oxygenates potential in affecting PN emissions. Both PFI and DI injection strategies were investigated in this campaign.

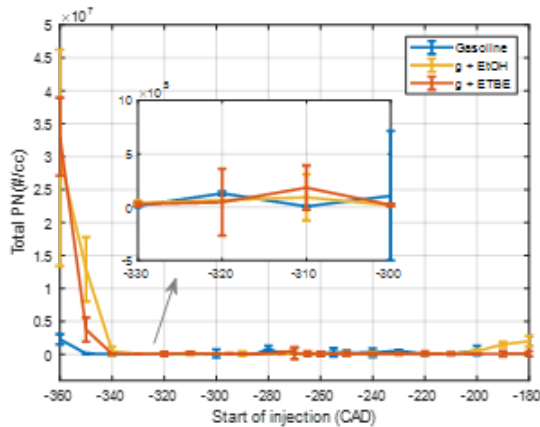


Figure 5.3: *Effect of start of injection (SOI) and fuel blends on raw exhaust PN at lower load of 4.5 bar IMEP and 2000 rpm [22]*

It is unlikely to have wall wetting at low load in DI, so the PN emissions for all the tested fuels were expected to be similar under these conditions. This behavior is further

confirmed by the results from SOI timing optimization that was done to minimize PN emissions in DI mode (Figure 5.3). However, Zhang et al. [75] found that oxygenate addition, in general, hinders the formation of soot precursors, which can ultimately reduce PN as observed here at low loads. Larger amounts of fuel must be injected at high load, which influences the impact of wall wetting as seen from higher PN levels at high load (Figure 5.4). The blend g+EtOH gave higher raw as well as solid PN compared to the other blends. The blend g+ETBE gave similar PN as the reference fuel non-oxygenated gasoline. As the particulate diameter goes down, the PN from g+ETBE gets substantially lower compared to other fuel blends, especially PN < 23nm. The oxygenated fuel blends have relatively higher density than non-oxygenated gasoline which can lead to higher PN [61]. The consistency of results from DI and PFI tests suggest that slight changes in fuel properties do not greatly contribute to PN formation. However, impact from fuel effects was found to be stronger in DI mode at low loads.

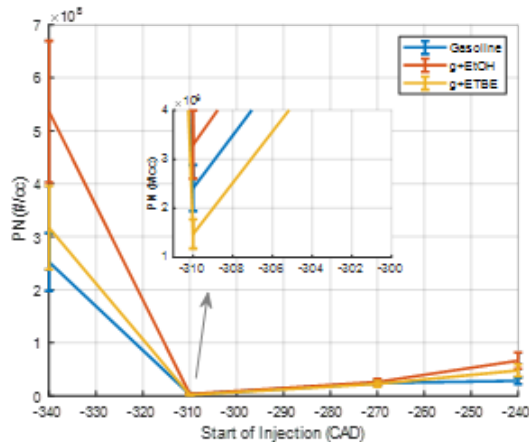


Figure 5.4: *Effect of start of injection (SOI) and fuel blends on raw exhaust PN at a higher load of 9 bar IMEP and 2000 rpm [22]*

Large quantities of low-diameter (i.e. sub23 and nucleation mode) particulates were formed under all tested conditions. Consequently, exhaust samples were passed through a thermodenuder to remove volatiles and enable measurement of solid PN emissions, in accordance with the PMP protocol. At low load (4.5 bar IMEP), both the oxygenated blends emitted the lowest solid PN, while the reference non-oxygenated gasoline generated the lowest solid PN emissions at the higher load of 9 bar IMEP. The robustness of protocols for measuring legislated PN emissions is highly dependent on the ability to accurately measure solid PN emissions. However, artefacts are common when measuring solid PN, so it is important to consider both total and solid PN emissions to properly understand the effect of fuel properties. Oxygenated fuel blends provide a good way of reducing PN emissions in raw exhaust because most passenger vehicles are mainly driven under partial

load. However, under high load conditions, non-oxygenated gasoline emits lower PN. The results obtained with the oxygenated blends indicate that oxygenates in fuel may reduce PN emissions by increasing the rate of soot oxidation. Moreover, oxygenates have the opposite or low effect at high load, presumably because of a possible increase in the formation of polycyclic aromatic hydrocarbons (PAH), which act as soot precursors [62].

Generally, when more fuel is injected at higher loads, it is virtually impossible to avoid liquid fuel hitting other combustion surfaces such as the cylinder liner or cylinder head. In accordance with the argument made above, this increases liquid contact with combustion surfaces, which increases PN emissions for oxygenated fuels more than it does for gasoline. Therefore, PN formation is expected to increase with the load, and this effect is strengthened as the fuel's oxygenate content increases. There are thus multiple competing mechanisms affecting PN formation whose relative importance may differ between engines. Consequently, it is unsurprising that the trends reported in the literature are inconsistent. At the higher tested load of 9 bar IMEP, the PN and SPN emissions from the tested engine were 4-6 times higher than those observed at the low load, depending on the fuel type.

The trends in SPN emissions differed markedly from those for raw PN, especially for oxygenated blends in the sub23 size range. Additionally, the relative contribution of solid PN to overall PN emissions appears to depend on the choice of oxygenate and the engine operating conditions. These results clearly show that adding oxygenates to gasoline (at least up to 22% v/v) does not reduce SPN emissions. Blends with much higher oxygenate contents such as E85 will always dramatically reduce PN emissions because they cause oxidation to clearly dominate over formation. However, the use of higher oxygenate contents was not possible in this work because the blends had to comply with the EN228 standard.

## 5.2 Particulate formation and visualization

The later part of the PhD thesis studied particulate formation in GDI by combining optical investigation with engine exhaust measurements. In this part, cold starts and warm-ups were first studied at lower loads and then extended to higher loads. Although, higher loads were considered in the first part of the thesis to study basic phenomena that cause PN formation, the insights and observations thus realized were carefully adapted for visualization studies in the second part. The highest particulate emissions during a driving cycle occur under cold-start, warm-up, and load transient conditions (see Figure 2.1). These challenging areas of drive cycle is thoroughly considered and investigated along with optical visualization to determine further understanding on PN formation.

### 5.2.1 Identification of soot sources during warm-up

This particular experimental campaign focuses on PN emissions and sources of PN formation in warm-up stages, which have received limited previous research attention, and effects of varying coolant and oil temperatures on PN emissions and associated processes, which must be elucidated to reduce toxic emissions during warm-up. The behavior of small particles is regarded as particularly important for meeting future legislative requirements. A high-engine speed was selected for the tests to ensure that the engine operation was stable and the warm-up process fast. Sizes and numbers of particles were recorded, and the combustion was visualized using an endoscope connected to a high-speed camera. Engine coolant and oil temperatures were varied between 15 and 90°C to mimic warm-up conditions. In addition, effects of delaying the start of ignition (SOI) on the emissions in these conditions were examined. The experimental setup is described in the next section.

Figure 5.5 shows effects of varying coolant and engine oil temperature, individually, on particulate emissions. PN emissions were found to decline dramatically with increases in coolant water temperature at a fixed oil temperature of 15°C. In contrast, increases in oil temperature had no significant effect on PN with the coolant water temperature set at 15°C. Previous studies of effects of varying coolant temperatures on particulate emissions [28, 29] have found similar effects of coolant water temperature on PN; the warmer the coolant, the better the combustion and lower the PN emissions. Clearly, as coolant water is in contact with much of an engine's cylinder head its temperature profoundly affects temperatures of the combustion chamber surfaces, and hence PN emissions. Note that while one temperature was varied the other was kept cold (at 15°C) to relate the results closely to cold start conditions. However, small amounts of engine oil enter the combustion chamber with movements of the crank shaft, thereby contributing to some PN. This is unlikely to have significantly affected PN emissions when the engine oil was cold (Figure 5.5), but it still made some contribution to PN emissions, so coolant and engine oil were varied together for the rest of the thesis. Hereafter, coolant temperature refers to both coolant and engine oil temperatures.

Although, this thesis mainly focuses on particulate emissions, standard emission measurements were almost always recorded along with PN and images in all the experiments.



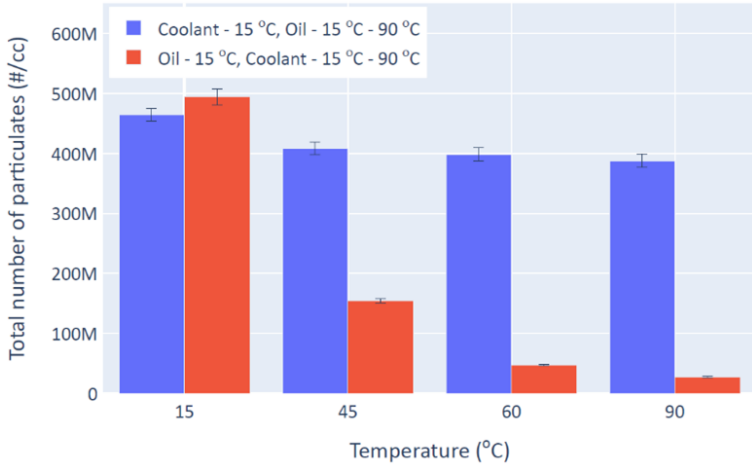


Figure 5.5: *PN concentrations recorded with indicated coolant and engine oil temperatures,  $-310$  CAD injection timing and 200 bar injection pressure. 1000 rpm/ 4.5 bar. The error bars correspond to  $\pm$  one standard deviation [43]*

It showed fuel consumption (FC) and gaseous emissions recorded at the selected coolant temperatures. FC and HC emissions were found to behave in a similar fashion, decreasing with increases in coolant temperature, summarized in Paper III [43]. These observations are found to be consistent with previous findings in literature [6, 61].

## Coolant Temperature and Injection Timing

Figure 5.6 shows that varying injection timing significantly influenced soot sources in terms of luminosity. Generally, as observed in Figure 5.5, PN dramatically declined as coolant temperatures increased. Higher coolant temperature will lead to warmer cylinder surfaces that enhance evaporation of fuel films, so the in-cylinder mixture can become richer, which balances the reduction in pool fires due to warmer surfaces. If more fuel films evaporate, the combustion of liquid fuel films will decrease, so the abundance of large particles will decline. This is evidently observed at  $90^{\circ}\text{C}$  at all tested injection timings in Figure 5.6.

To enhance the visualization of the flames' statistically verified locations in the combustion chamber, the relative frequency images were then superimposed on a gray illuminated background (the camera view). The image analysis used for generating the relative frequency images is detailed in section 3.2.3. The results are presented in Figure 5.6 for all temperatures and injection timings. At an injection timing of  $-310$  CAD there was generally a lot of diffusion flame on the piston top at coolant temperatures between 15 and  $45^{\circ}\text{C}$ . In the middle of the piston top, diffusion flame can be seen in more than 40% of the single shot images. At  $60^{\circ}\text{C}$  the diffusion flames were starting to decrease and at

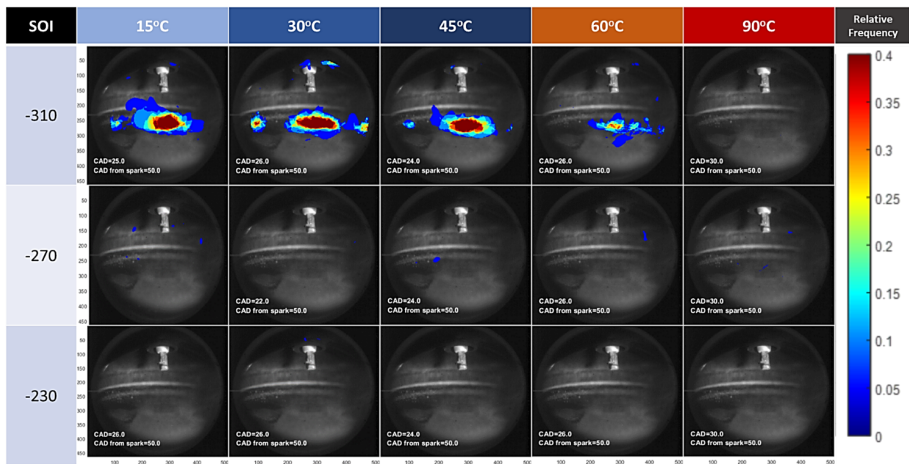


Figure 5.6: *Relative frequencies of diffusion flames occurrence calculated from analyses of images of 20 combustion cycles at 50 CAD after ignition. Engine speed 1000 rpm, IMEP = 4.5 bar [43]*

90°C no diffusion flame can be seen. Thus, diffusion flames on the piston clearly decreased with increases in temperature, especially beyond 60°C. This is because remaining liquid fuel film on the piston did not vaporize and mix in time at the lower temperatures. In the experiments with this engine, the injection timing of  $-310$  CAD resulted in the lowest PN emissions. Earlier timing would have increased the diffusion flame on the piston and later timing would have impaired the mixing quality. Clearly, coolant water temperatures lower than 90°C resulted in dramatically higher PN emissions by promoting formation of pool fires and diffusion flames on the piston, thus the piston top temperature was also decreased by the lower coolant water temperatures.

The idea was to measure PN and identify sources of soot formation in an internal combustion engine during warm-up. Under conditions other than those tested in the paper, such as increasing speed and load would influence PN because higher engine speed increases the distance between the liquid spray front and the piston, but on the other hand mixing time decreases. Since the result indicate that the main source of soot formation is liquid fuel on the piston therefore, PN could decrease at higher engine speeds by decreasing piston wetting. In this paper, similar mechanism was achieved by delaying injection at fixed speed to minimize piston wetting which in turn resulted in decreased PN. With increased load, injected amount of fuel increases hence can result in higher PN.

Thus, stationary operating points were used to provide a clear overview of warm-up phenomenon. Warm-up in a vehicle would provide a realistic time variation in coolant temperature which is not the same as stationary operating points. However, studying PN formation and emissions at stationary points is still valuable for overall understanding of PN under warm-up conditions.

## 5.2.2 History effect of soot formation on PN emissions

So far in the thesis, experiments have shown that liquid fuel impingement on the piston top is a major contributing factor to high PN emissions: avoiding this can reduce the emissions by more than an order of magnitude. The most effective way to avoid fuel film formation on the piston is by using an SOI timing that allows the piston to move sufficiently far from the top dead center (TDC). Injection timings that are too early can lead to fuel impingement on the piston, and this increases soot formation. However, an SOI timing that is too delayed can result in poor mixture quality and, again, lead to high PN especially at high loads when large volumes of fuel are injected into the cylinder as observed in previous SOI sweeps (see Figure 5.4).

This experimental campaign focuses on the causes of poor repeatability of PN measurements in engine testing of the type usually undertaken in engine control unit (ECU) calibration and research and development. The primary purpose was to consider the effects of the cycle-to-cycle variations and engine state (as encountered when varying SOI timing) on PN emissions. For this set of experiments, the engine thermal condition derived from all the phenomena associated with SOI, such as fuel film, a cooler piston, spray cooling, slower evaporation of fuel from the liquid film, and mixture quality, is called an engine state. The influence of a preceding engine state on the following engine states is termed a history effect. Several experiments were carried out where SOI was changed over a certain number of cycles and the engine state determined.

SOI affects the amount of time available for the fuel to mix with air in the cylinder, which later influences mixture homogeneity and combustion. Two extreme SOI timings leading to a maximum difference in PN were used:  $-310$  CAD and  $-340$  CAD. At an injection timing of  $-340$  CAD, significant numbers of fuel droplets hit the piston since the distance between the injector and the piston top land is short. This leads to a cooling of the piston [13] by at least 5 degrees, with the formation of a liquid fuel film dependent on liquid volume, heat of vaporization of the fuel, load, SOI, etc. Later this liquid film slowly vaporizes. If a liquid film remains on the piston at the start of combustion, this leads to slow-burning diffusion flames on the piston top, which remain for a significant time, often over 60 CAD. This greatly contributes to particulate formation and is undesirable. Normally in combustion engines, most of the particulates formed are oxidized, but when this happens late in the combustion event, the oxidization rate is low since the pressure and the temperature in the cylinder reduce rapidly during the expansion.

Although stoichiometric conditions are recorded by the oxygen sensor in the exhaust for both cases, the local in-cylinder fuel-to-air ratio can be significantly different due to the presence of liquid fuel on the piston. Fuel-rich conditions in the vicinity of the piston top and global stoichiometry mean that there must be lean conditions existing elsewhere in the cylinder volume. Fuel-rich regions lead to high PN levels due to improper combustion. In this case, pool fires on the piston surface, much denser than the combustion at ignition, are formed.

SOI timing of  $-340$  CAD was found to produce high levels of PN due to the impingement of liquid fuel on the piston top, which was visualized as high flame luminosity. A slightly later timing of  $-310$  CAD, as expected, reduced the burning of the diffusion flames and produced lower levels of PN. Using these two timings, a dynamic test sequence was designed, as shown in the top part of Figure 5.7.

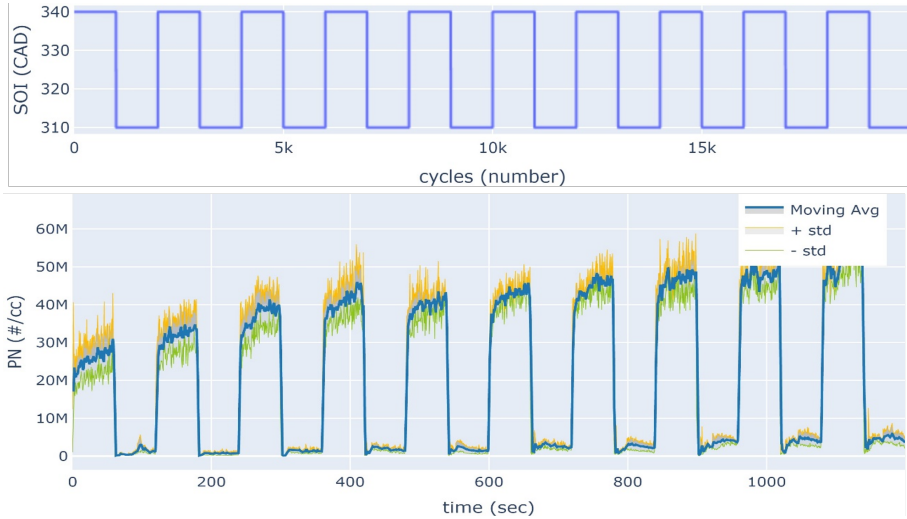


Figure 5.7: *PN emissions at 9 bar NMEP for 20,000 cycles and 2000 rpm with discrete step variation in SOI switching between  $-310$  CAD and  $-340$  CAD with 1000 cycles for each timing [76]*

The DMS500 instrument can repeatably capture changes in PN levels every half a second and as soon as there is a change in SOI. Each SOI was maintained for 1000 cycles (60 sec) and the sequence was repeated over five times. When running the  $-340$  CAD SOI setup for 1000 cycles, there is insufficient time for the fuel film formed in one cycle to evaporate before the next cycle, resulting in piston deposits that will build up within these 1000 cycles. Comparing the PN levels from the final cycle (1080 sec) with the first cycle (0 sec) clearly shows an increase to approximately double the PN, thus confirming the existence of history effects on PN.

In the following sequence, the SOI timing was gradually changed from  $-180$  CAD to  $-340$  CAD over 10,000 cycles in steps of 0.016 CAD per cycle and then back to  $-180$  CAD, in a total of 20000 cycles. Each SOI timing lasted exactly one cycle before changing. One advantage of a continuous SOI sweep is that it minimizes changes in combustion, and therefore, sudden changes in the PN data are unlikely to be seen. The results from the continuous SOI sweep are shown in Figure 5.8. The PN levels are quite symmetric except at around  $-340$  CAD. The asymmetric behavior of the  $-340$  CAD peak indicates the presence of the history effect. The history effect here is weak and does only occur

for SOI timings where impingement is high. The reason for the shorter duration of the history effect is that impinging conditions occur for fewer cycles here than in the sequence shown in Figure 5.7. The lowest PN levels are observed at  $-180$  CAD and  $-310$  CAD. For injection timings later than  $-320$  CAD, there is no fuel impingement on the piston. This means that if mixing time were the most influencing factor for PN levels, then  $-180$  CAD should have a higher PN than at  $-310$  CAD.

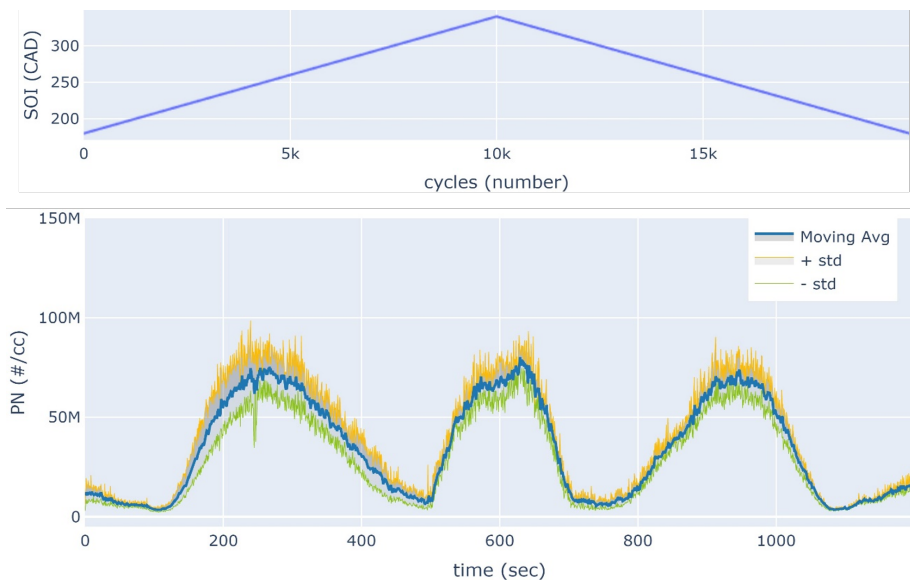


Figure 5.8: *PN emissions at 9 bar NMEP for 20,000 cycles and 2000 rpm with linear continuous variation in SOI changing from  $-180$  CAD to  $-340$  CAD and back to  $-180$  CAD with accurately predefined timing for each cycle.[76]*

The higher PN levels appear at three peaks with similar levels and correspond to  $-250$ ,  $-340$ , and again  $-250$  CAD. The high PN at  $-340$  CAD is due to pool fires and correlates with the data shown in Figure 5.7. At  $-250$  CAD, however, the higher PN cannot be due to the lack of mixing time since the timing of  $-180$  CAD gave a much lower PN. The  $-250$  CAD peaks are almost symmetrical for both occurrences, in both shape and quantity. Contrary to data shown in Figure 5.7, the symmetry of PN levels from the start to the latter half of this sweep is due to the significantly shorter time for deposits to form and the history effect to occur. It is noteworthy that, with a continuous change in SOI timings, the PN levels at  $-340$  CAD, which is clearly a state where deposits form, and at  $-250$  CAD are roughly similar. Combustion images from 10 cycles around these SOI timings were captured to study the PN sources at these timings. Images at  $-310$  CAD were also taken to ensure that the sequence produced reliable results in comparison with previous sequences. These are shown along with a frequency analysis in Figure 5.9.

The reason for high PN at  $-250$  CAD can be identified from the images in Figure 5.9 as soot formed in fuel-rich zones due to poor mixing, confirmed here with endoscope

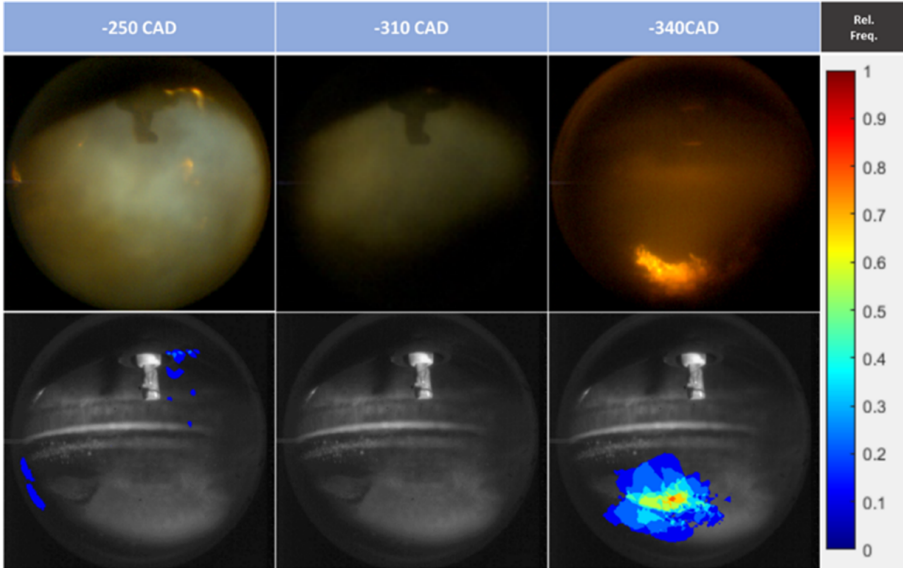


Figure 5.9: *Single-shot images of the combustion chamber from one of the combustion cycles at 35 CAD during engine operation at an SOI of  $-250$  CAD,  $-310$  CAD, and  $-340$  CAD, respectively, at 9 bar NMEP and 2000 rpm. Bottom row shows the relative frequency.[76]*

images and image processing. Advancing SOI in this sequence also produced a decrease in PN until around  $-310$  CAD. This meant that there was no diffusion flame due to poor mixing with this timing, resulting in favorable PN levels as seen in Figures 5.8 and 5.9. As the SOI reached the second peak at  $-340$  CAD, impingement was dominant and seen mostly on the piston top. Thus the peak at  $-250$  CAD is related to unfavorable timing and mixing relative to the in-cylinder air motion (tumble motion) at this specific load and speed.

Sudden changes in a dominant influencing parameter, such as SOI, clearly affects PN. Consequently, the sequence with the smallest SOI variations between cycles (Continuous SOI sweep) resulted in the smoothest changes in PN data. For this sequence, the PN data showed two distinct peaks indicating two unfavorable SOI timings at  $-250$  CAD and  $-340$  CAD that produced excessive soot formation. To analyze the particulate source for the different SOI timings further, in-cylinder combustion was visualized with an endoscope connected to a high-speed camera. The source was found to be soot formation due to fuel-rich zones forming as a result of poor mixing and heavy deposits on the piston top at  $-250$  CAD and  $-340$  CAD, respectively. This occurred for multiple repeats, and indeed, there was symmetry between PN levels and SOI timings across the different types of SOI sweep used. In the vicinity of the timing at  $-340$  CAD, PN levels were always seen to have an increasing slope, indicating heavy piston wetting.

When the SOI timings were varied in steps (Discrete SOI sweep), the data were remarkably different with no symmetry. Overall, the PN behavior mirrored the continuous sweep, with  $-250$  CAD and  $-340$  CAD causing peaks in PN levels. However, there were significant variations in PN levels within multiple repeats of any given SOI, proving the existence of the history effect. Similarly, randomization of the SOI timings gave further insights into the extent of the history effect on PN. History effect on PN occurs for early fuel injections where there is a lot of fuel impingement. If the remaining fuel film leads to diffusion flames on the piston, and yet the lambda sensor in the exhaust shows a stoichiometric mixture, the air-fuel mixture in the cylinder must be lean. Therefore, if the PN from diffusion flames on piston top is excluded, then PN from incomplete combustion of the bulk mixture should be lower than stoichiometric. Possible imperfections in the mixture under lean conditions do not tend to result in rich zones producing more soot. Therefore, spray piston impingement may be the root cause of higher PN. Moreover, this piston impingement leads to diffusion burn with high PN formation, which in turn leads to deposits on the piston. These two phenomena together cause history effect on the upcoming cycles. History effect can be minimized by avoiding impinging rather depositing conditions or at least being run for a long time if not avoidable.

### 5.2.3 Visualization of soot sources during cold transients

In general, gasoline engines should be operated under stoichiometric conditions to limit emissions of pollutants such as THC, NO<sub>x</sub>, CO, and particulates. Unfortunately, stoichiometric operation cannot be maintained when the load increases suddenly, causing particulate emissions to spike during load transients [77, 78]. Future emissions standards will impose limits on particulate emissions when engines are operated at sub-optimal temperatures (including during cold starts), making it essential to study emissions under such conditions. It is particularly important to consider the impact of load transients during operation at low temperatures because the combined impact of the two conditions has the potential to generate extremely high PN emissions.

Following each load transient, the engine was operated at the higher load of 12 bar NMEP for a relatively long time (3 minutes) to enable measurement of PN emissions under stabilized stationary conditions (see Figure 3.6). Figure 5.10 shows the PN measurements at the end of the stationary period for each experimental set. Factors that significantly influence PN formation include the formation of wall films due to fuel impingement on combustion chamber surfaces such as the piston top, and mixing, which depends on the SOI timing and its interaction with the air motion [79]. Figure 5.10 shows that PN emissions in the late injection (−270 CAD) case are significantly higher than in all other cases when the SOI timing was −310 CAD. Because late injection should reduce wall film formation [79], the increased PN emissions in the late injection case must be due to shortened mixing times and less favorable interactions between the fuel spray and the air motion in the cylinder.

### PN during load transients

Figure 5.11 shows PN emissions during the set 1 load transients, which are treated as a baseline for comparison to all of the other conditions examined in this work. In general, PN emissions declined dramatically as the coolant temperature increased. This temperature dependence is very similar to that seen under stabilized conditions (see Figure 5.10). As in the steady state case, PN emissions at 90 °C were significantly lower than at all other tested temperatures during the load transient.

Note that the transient occurs over just a few seconds, so that the number of PN samples per experiment was limited. Therefore, despite performing replicate experiments, there was too much variation in the measured PN emissions to quantitatively characterize trends at lower temperatures. As expected, PN emissions peaked during the transient at all temperatures, and the peak value decreased significantly as the coolant temperature increased. Variation of the other parameters listed in Table 3.4 had only minor effects, indicating that the influence of these parameters on PN emissions is dominated by that of the coolant temperature. To obtain visual evidence on soot formation sources and their location in the cylinder under different experimental conditions, combustion imaging was performed. If fuel film is the dominant factor governing PN emissions [6], the presence of yellow flames should correlate strongly with the measured PN emissions.



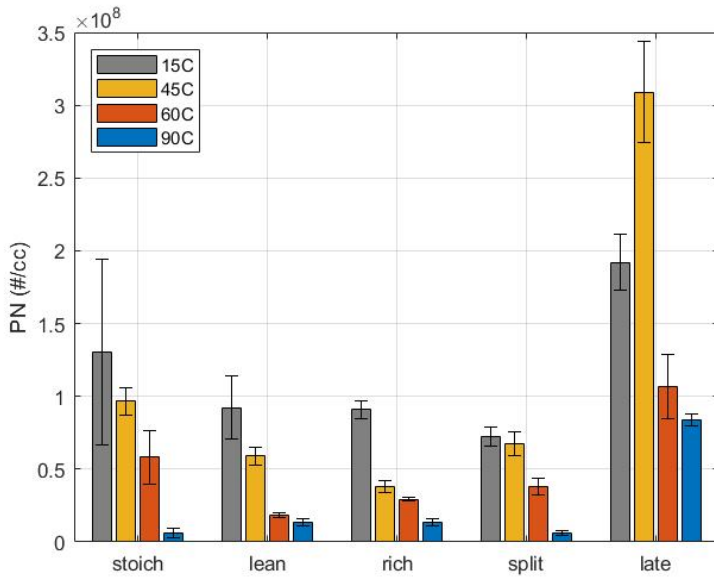


Figure 5.10: *Post-transient PN measurements during stable operation at 12 bar NMEP at the end of the routine presented in Figure 3.6 for different experimental sets and coolant temperatures.*

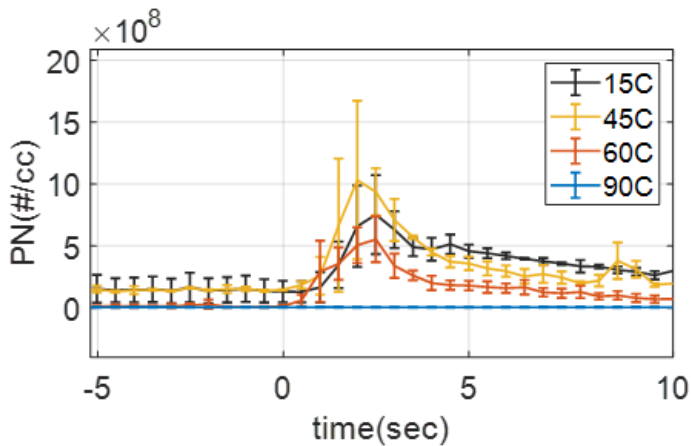


Figure 5.11: *PN measurements over time at different engine coolant temperatures during the load transient routine shown in Figure 2. SOI = -310 CAD, engine speed = 2000 rpm, lambda = 1.*

Figure 5.12 shows single shot combustion images during the load transients whose PN emissions are plotted in Figure 5.11, followed by images acquired during stable operation at the higher load after the transient. All of the images were captured at 50 CAD after ignition ( 30 CAD after TDC), which is close to the timing of maximum diffusion flame luminosity. At coolant temperatures of 15°C and 45°C, the images clearly show a predominance of diffusion flames resulting from liquid fuel impingement on the piston head as well as some fuel rich zones near the valves. As the load transient progresses, the extent of the diffusion flames increases significantly, and the images start showing saturation at 10 bar NMEP, indicating high soot levels. After 3 minutes of operation at 12 bar NMEP, the images are very dark due to heavy sooting on the window. The saturation of the images captured towards the end of the transient sequences was due to the use of a fixed lens aperture that was adjusted to visualize soot sources during the first part of the transient. At higher coolant temperatures, the piston top becomes warmer, which facilitates fuel film vaporization and thus reduces the formation of diffusion flames. Accordingly, almost no yellow flames are visible during the transient when the coolant temperature is 90 °C, in good agreement with the PN emissions data presented in Figure 5.11.

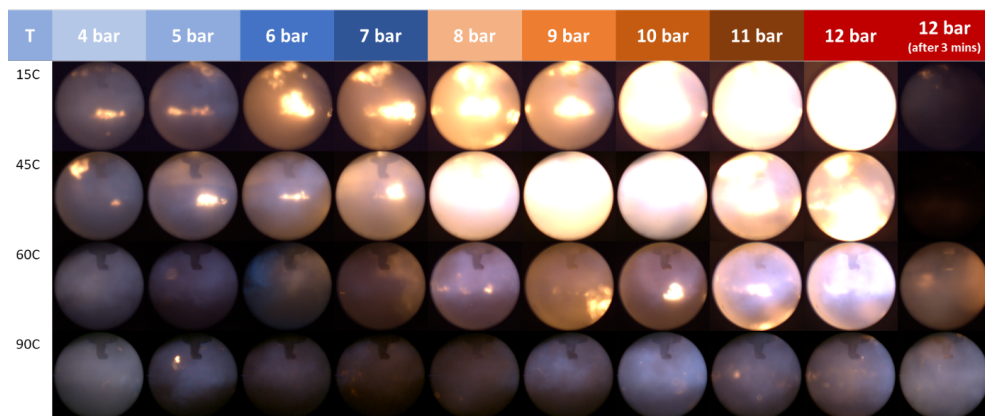


Figure 5.12: *Single-shot images at 50 CAD from ignition during a load transient in which the load increases from 4 to 12 bar NMEP. The final column shows images after sustained operation at 12 bar NMEP. SOI = -310 CAD, engine speed = 2000 rpm, A/F =1. Each row shows an image captured during a single experimental replicate at the indicated coolant temperature. The incidence of diffusion flames clearly decreases with increasing temperature. Figure 5.11 shows the corresponding PN emissions.*

It is generally difficult to distinguish between yellow flames arising from impingement on the piston and those originating from other soot sources such as poor mixing on the basis of single shot images alone. Two criteria must be satisfied to confidently state that soot originates from impingement on the piston: yellow flames must be observed at the same location in all replicates for a given set of experimental conditions and the extent of the yellow flames at this location should decrease when the SOI is delayed [6]. The

results of a frequency analysis based on the images shown in Figure 5.12 are presented in Figure 5.13. In the first part of the transient (between 4 and 9 bar NMEP), the main soot sources are at the piston top at the lower coolant temperatures of 15 and 45 °C. At higher loads, high yellow flame frequencies become more widely and inconsistently distributed within the cylinder, implying that impingement has become less significant and that soot formation is mainly due to poor mixing. At 60 °C, the extent of yellow flames was greatly reduced, and they were almost undetectable at 90 °C. The occurrence of diffusion flames thus clearly fell as the coolant temperature increased, especially above 60 °C. The temperature dependence of soot formation seen in the images thus agrees well with the PN data presented in Figure 5.11.

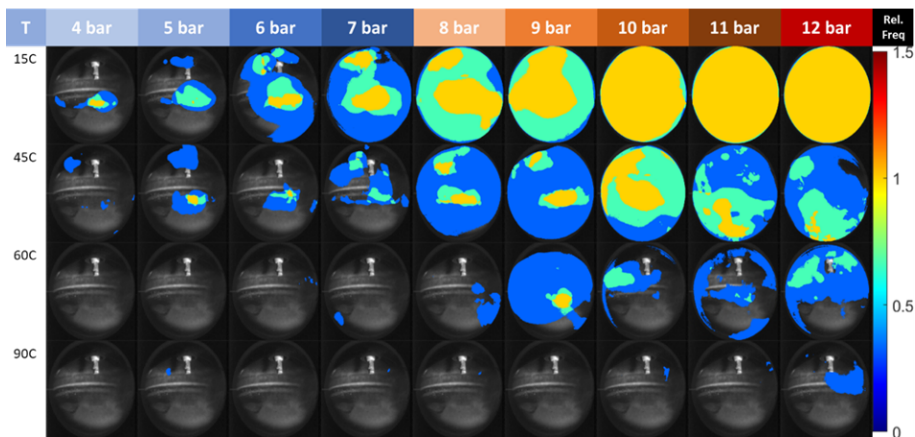


Figure 5.13: *Relative frequencies of yellow flames at different locations in the cylinder during the set 1 (baseline) transients at 50 CAD after ignition. SOI = -310 CAD, A/F = 1, speed = 2000 rpm. Raw images are shown in Figure 5.12.*

The tested conditions correspond to the transients that occur during engine warm-up, which are associated with very high PN emissions. Under all of the studied conditions, PN emissions at low coolant temperatures were substantially lower than at a coolant temperature of 90 °C. The coolant temperature is thus the dominant factor governing PN emissions during warm-up load transients.

At low load, delaying the SOI reduces wall-film formation [43] and thus reduced soot formation during the early parts of the transient. However, at the higher loads towards the end of the transient, delayed injection adversely affected the fuel spray's interaction with the air motion, leading to worse fuel-air mixing and a significant increase in PN emissions. A more fine-grained sweep of the SOI delay could potentially have revealed an SOI timing that improved mixing and reduced PN emissions, however. These results also suggest that cylinder heads should be designed to enhance mixing effects that improve interactions between the fuel spray and air motion if delayed injection strategies are to be used. Split injection reduced soot formation, especially in the later parts of the transient.

The air-fuel ratio had only a minor influence on PN emissions when compared to the coolant temperature and injection strategy.

Visualization with endoscope in a metal engine is a straightforward method for identifying the locations of soot sources, although endoscope images should be complemented with simultaneous PN measurements. However, endoscope images are much less useful for studying mixing-related soot sources because such sources move randomly in the cylinder, resulting in a low relative frequency of sooting flames even when PN emissions are high.

## 5.2.4 Effect of fuel on PN during load transients

This section is an extension of the investigation presented in the previous section, with an intention to study the effect of fuel by testing gasoline blends with higher percentages of oxygenates such as EtOH. These results were obtained at the end of the thesis and are not published in any journal or conference at the moment.

The transients in load comprising of sudden changes in engine load is a complex phenomenon where a lot of parameters are at action influencing the in-cylinder combustion characteristics which in turn affect PN emissions. Extending the skills required to conduct an engine transient, the same technology has been used with gasoline and ethanol blends to study the PN behavior. Two fuel blends have been used to evaluate the effect of fuel on PN during transients. Both are gasoline blend with 20% ethanol and 85% of ethanol to help understand the effect of oxygenates on the soot formation in the combustion chamber. So far, in literature, studies have found that the oxygenates help in soot oxidation post formation which leads to lower PN emissions in the engine exhaust. However, there are negative effects associated with increased heat of vaporization in the blend that leads to slower evaporation of fuel from the formed fuel films, if any, on the cylinder surfaces.

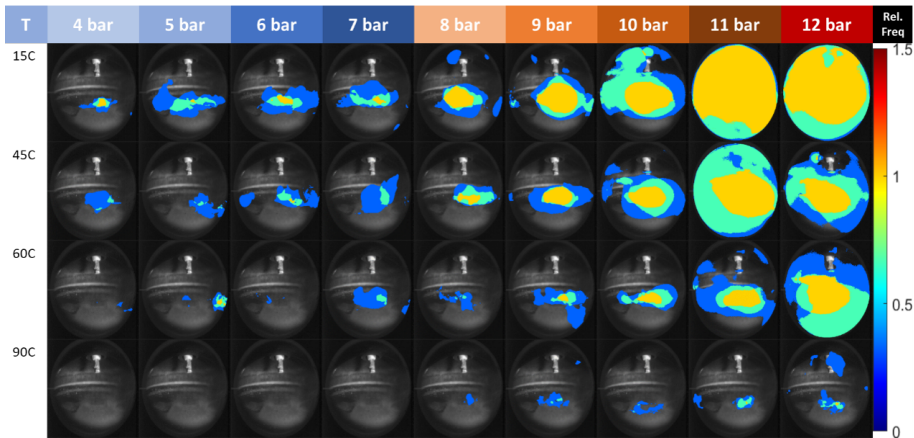


Figure 5.14: *Relative frequencies of occurrence of diffusion flames calculated from analysis of images from multiples repeats of the load transient at 50 CAD after ignition using fuel E20.*

Comparing Figures 5.13, 5.14 and 5.15 shows that the extent of yellow flames have significantly come down with the introduction of oxygenates into the fuel blends. Even with as little as 20% EtOH, the yellow flames have started to disappear from loads 6-9 bar IMEP. They are no yellow flames to be seen in E85 upto 9 bar IMEP at all engine coolant temperatures in all the load transients.

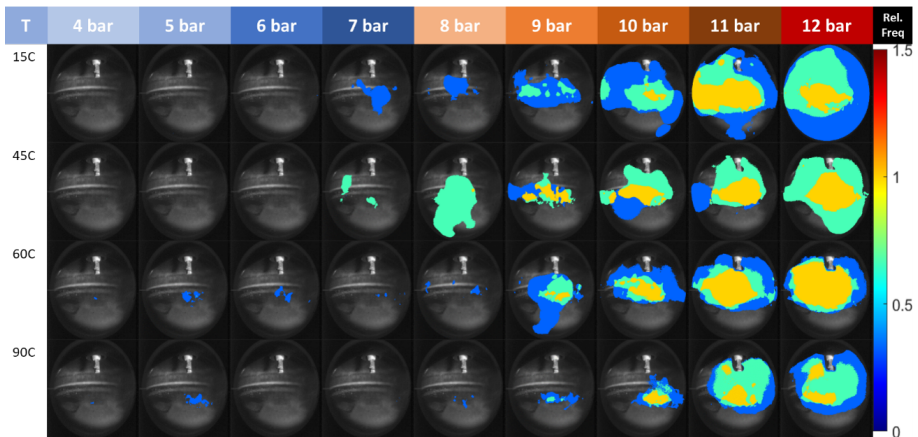


Figure 5.15: *Relative frequencies of occurrence of diffusion flames calculated from analysis of images from multiples repeats of the load transient at 50 CAD after ignition using fuel E85.*

# 6 Conclusions

There is a significant potential to reduce the overall PN formation in a GDI engine with a combination of studied strategies. For one, GDI engine equipped vehicles operating at high coolant temperatures can significantly reduce the overall PN emissions throughout a drive cycle including warmup and transients. Further reduction is possible with operating at optimized later injection timings. PN reduction is further ensured by making sure that the engine is run in near stoichiometric conditions. Additionally, higher coolant temperatures also enables improved combustion efficiency along with improved fuel consumption. Secondly, with the novel cRIO controller developed for cycle-to-cycle control, the opportunity of identifying and quantifying reduction strategies in fast phenomena such as load transients and history effect along with endoscope images, adds to the overall knowledge on soot formation and particulate emissions. The research questions have been addressed by five major campaigns that have provided insights into particulate formation in GDI engines. The obtained results have led to the conclusions listed below. Additionally, outstanding challenges related to particulate formation and emissions are discussed.

## **Does controlling homogeneity of the charge mixture using dual injection help with reducing PN formation?**

GDI engines do not unconditionally benefit from improved mixture formation due to direct injection when it comes to particulate formation at high loads. Especially, when compared with its counter-part technology PFI where the fuel is injected in the inlet valve. Particulate emissions heavily depend on combustion quality and it can be significantly improved by homogeneity of the charge mixture. With a control on homogeneity of the mixture by manipulating the fuel injected through PFI/DI could reduce PN up to 10-fold while modestly increasing fuel consumption. PN reduction was possible by benefiting from the advantages each PFI and DI add to the engine individually such as improved mixing and efficient combustion with lower fuel consumption respectively. Moreover, Solid PN i.e., exhaust sampled through a VPR also decreased almost linearly as the upstream PFI contribution increased but was independent of engine speed.

## **What advantages does extra oxygen content in the fuel offer considering PN formation and emissions?**

Oxygenated fuel helps in reducing PN from combustion mainly by replacing some of the carbon content in the fuel with oxygenate molecules. Increasingly varying oxygenated content (upto 22% v/v) in the tested fuel blends gave further insights into PN emissions. Adding oxygenates upto the tested percentile did not affect solid PN significantly. With an SOI sweep, PN emissions were found to be very sensitive to SOI timing. The most significant differences in SPN between fuel blends occur when the sprays hit the wall at very early SOI timings. At very early SOI timings, oxygenated fuel blends dramatically increase both PN and SPN due to increased injection duration. However, studying

the blends at low load gave more insights into possible PN reduction. At low loads, oxygenated blends reduce raw PN almost four-fold. From this study, it was evident that higher percentages of oxygenates are required to see a potential reduction in PN. This observation was further validated by transient studies performed at the end of the thesis when E85 was tested and compared against standard gasoline (G95).

### **What insights does locating sources of soot offer considering reduction of PN during the warm-up?**

Diffusion flames play a big role in PN emissions as they are a result of poor combustion, fuel rich zones and carbon rich emissions. Using endoscope images to locate soot sources, especially yellow diffusion flames as a result of plank's radiation helped identify the potential of reducing PN at warmup. Engine warmup is definitely a focus area when it comes to any drive cycle of a GDI engine where there is exceptionally high levels of PN emitted. In this study, the main source for soot formation was identified to be on the piston top at warmup. Total PN declines dramatically with increases in coolant temperature, especially at temperatures higher than 60°C, beyond which PN emissions stabilized and were not affected by further temperature increases. High frequency of yellow flames in the images was strongly correlated with diffusion flame occurrence and PN emissions. Taking into account that SOI has a significant influence on PN from the previous study, soot reduction during warm-up was achieved by retarding SOI timing even at colder coolant conditions. Later fuel injection timings reduced total PN emissions in warming-up conditions due to the associated reduction in wall films on the piston. The decrease was mainly in numbers of small particles. Bigger particles were also found to be sensitive to injection timings, but only in relatively warm conditions. Total PN emissions declined as coolant temperatures increased and less diffusion flame formed, as clearly seen in endoscope images. As expected, no diffusion flame was observed at later injection timings, which also explains the decrease in PN emissions.

### **Is there any history effect on PN formation and emissions?**

As part of this work, a novel cRIO controller was developed to investigate soot formation in each cycle of operating of the GDI engine. This controller helped control injection timing, duration, ignition and throttle to ensure stoichiometric, rich or lean operation with good combustion phasing in each cycle. Using this controller, it was possible to study the effect of previous engine thermal conditions on soot formation. This phenomena was further tested, quantified and is established as history effect of PN. History effect on particulate formation using a cycle-to-cycle deterministic variation of engine parameters, particularly SOI timing. SOI timings were changed in real time or online according to different preprogrammed 20-minute-long deterministic sequences. The history effect is evident for early SOI, under spray-piston impinging conditions where liquid fuel film is present resulting in deposits and high PN. The data shows that PN can be very different depending on the order in which SOI is varied. PN was found to be almost equally high for impinging conditions (early SOI at  $-340$  CAD) and for later SOI timing (at  $-50$  CAD). The longer the duration of impinging conditions results in a stronger history effect.



## **Does any of the control mechanisms developed so far help reduce soot formation during load transients?**

Load transients are such fast events in a drive cycle, there is generally not enough time for the suddenly increased amounts of fuel to interact with the air and form a good mixture. PN measurements show high values due to sudden peaks caused by this poor mixing in every drive cycle analysis at transient conditions. In this study, a transient was carefully designed to run over 2 seconds to realize the potential of PN reduction strategies developed so far in this work. Both fuel films and poor air-fuel mixing were found to be important sources of soot during transients. The engine coolant temperature is the dominant factor governing soot formation during load transients. The second most influencing factor is the injection timing; delayed injection significantly increased PN emissions during load transients. Small variations in A/F had little effect on PN emissions during load transients. Under all tested conditions, soot formation was substantially higher when the coolant temperature was 15 °C than when it was 90 °C. Most soot formation occurred during the late (high load) part of the transient. A split injection strategy reduced PN emissions in the high load part of the transient. Qualitative changes (increases/decreases) in PN emissions can be identified from images when soot formation is dominated by wall films but not when it is mixing-dominated. PN emissions were higher during load transients than during stable operation at high load.

## 6.1 Novelty of the Research

The main objective of this thesis is to isolate the soot formation mechanisms that occur during combustion process and develop control strategies to reduce PN by eliminating these mechanisms. Even though many researchers have worked on reducing soot formation, very few studies have reported a clear structure of the formation process. Soot formation is in general, a complex phenomena which had multiple dependencies not only on the internal combustion engine parameters, but also on the ambient conditions. Ensuring good quality of combustion in each cycle is more or the less the main criteria for designing the efficient energy absorption system. The in-cylinder mechanisms which are heavily dependent on fuel-wall interactions in GDI are taken into consideration and found that heavy fuel-wall interaction leads to liquid fuel deposition on cylinder surfaces including piston top which leads to high concentrations of soot resulting in high PN in exhaust. Although, it is a well-established fact that wall-wetting leads to PN formation, this thesis achieves novelty by addressing the same in cycle-to-cycle detail, especially during fast events such as engine load transients.

Many researchers compared the effects of reducing wall-wetting by changing the start of injection and using alternative fuels on PN, especially gaseous kind in their work. Though there are similarities in literature, in the present work studying cycle-to-cycle combustion quality and wall-wetting, the existence of a phenomena affecting PN from previously run engine conditions, known as history effect was established. Quantifying history effect with duration of engine conditions definitely added to the understanding of soot formation in GDI engines.

Usage of visualization wherever possible added missing information that could otherwise result in faulty reduction techniques which are specific to certain measurement instruments. The detailed quantification achieved in this study is essential to developing soot reduction techniques as the world keeps moving towards a particulate/ pollution free biosphere.

## 7 Outlook and future work

All of the experimental work presented in this thesis was conducted using a standard metal GDI engine that was only modified by mounting an endoscope in the cylinder head. The aim of the work was to clarify the mechanisms of PN formation in GDI engines under conditions that generate high PN emissions and suggest ways in which such emissions could be reduced. While this was achieved, there are a number of strategies that could potentially deliver further reductions in PN emissions that were not examined such as increasing the direct or port injection pressure or using gaseous fuels. Another limiting factor of the conducted experiments was that the peak cylinder pressure in the experimental engine was restricted to 100 bar. Consequently, the highest loads examined in this work were below the high load ranges of some modern combustion systems, many of which can tolerate peak pressures of around 150 bar under the studied conditions. High load combustion is frequently associated with strongly sooting conditions due to a combination of fuel impingement and poor mixing. This caused extensive darkening of the engine's optical window, limiting the scope for detailed study of PN formation at high loads. One way to partially overcome this problem would be to use oxygenated fuels such as E85. All engine experiments presented in this thesis used gasoline with an octane rating of 95 (RON) aside from those using blends containing specific proportions of EtOH/ETBE. Another interesting fuel alternative that may solve some experienced issues is gas. Gaseous fuels like CNG could potentially eliminate wall wetting because they are not liquid. As such, they could be ideal fuels for high load combustion in highly efficient engines with zero particulate emissions. The author suspects that the objective of sustaining clean combustion at high load would be achieved if the load transient experiments presented herein were repeated using CNG or gaseous methanol as the fuel instead of gasoline.

Another interesting outcome of this work was the development of a novel cRIO controller that enables precise cycle-to-cycle control over engine parameters. By using this controller in conjunction with an electronic dynamometer to control engine speed, it became possible to conduct reproducible engine experiments on transients. Conducting more such experiments would enable optimization of the engine operating conditions to minimize engine-out emissions during transients and potentially eliminate the need for exhaust after-treatment. This could also be achieved by adopting carbon-free gaseous fuels such as hydrogen. However, a transition to gaseous fuels would require the use of cutting-edge technology for spark-ignition engines and would substantially increase the cost of the combustion system. In addition, the increasingly strict legislative requirements for high overall powertrain fuel efficiency mean that it may not be possible to produce cars without hybrid powertrains in the near future. If hybridization is enforced, the cost of the propulsion system would be increased further. The value of combining an expensive hydrogen combustion engine with a costly electric hybrid system may thus be questionable. This is a complex optimization problem that will have to be studied carefully to determine whether combustion engines will remain the dominant source of propulsion in cars.



# Bibliography

- [1] L. Chen, R. Stone, and D. Richardson. “A study of mixture preparation and PM emissions using a direct injection engine fuelled with stoichiometric gasoline/ethanol blends”. In: *Fuel* 96 (2012), pp. 120–130. ISSN: 00162361. DOI: 10.1016/j.fuel.2011.12.070. URL: <http://dx.doi.org/10.1016/j.fuel.2011.12.070>.
- [2] Marilena K. and Elias C. “Human health effects of air pollution”. In: *Environmental Pollution* 151.2 (2008). Proceedings of the 4th International Workshop on Biomonitoring of Atmospheric Pollution (With Emphasis on Trace Elements), pp. 362–367. ISSN: 0269-7491. DOI: <https://doi.org/10.1016/j.envpol.2007.06.012>. URL: <https://www.sciencedirect.com/science/article/pii/S0269749107002849>.
- [3] R. W. Atkinson et al. “Urban ambient particle metrics and health: A time-series analysis”. In: *Epidemiology* 21.4 (2010), pp. 501–511. ISSN: 10443983. DOI: 10.1097/EDE.0b013e3181debc88.
- [4] J. A. Bernstein et al. “Health effects of air pollution”. In: *Journal of Allergy and Clinical Immunology* (2004). ISSN: 00916749. DOI: 10.1016/j.jaci.2004.08.030.
- [5] B. Giechaskiel, U. Manfredi, and G. Martini. “Engine Exhaust Solid Sub-23 nm Particles: I. Literature Survey”. In: *SAE International Journal of Fuels and Lubricants* 7.3 (2014), pp. 2014–01–2834. ISSN: 1946-3960. DOI: 10.4271/2014-01-2834. URL: <http://papers.sae.org/2014-01-2834/>.
- [6] M. Raza et al. “A Review of Particulate Number (PN) Emissions from Gasoline Direct Injection (GDI) Engines and Their Control Techniques”. In: *Energies* 11.June (2018). DOI: 10.3390/en11061417.
- [7] Z. Erlangung and D. J. Bölter. “Auswirkungen von Ruß im Schmieröl von DI-Dieselmotoren auf das tribologische Verhalten und Tribomutationen von hochbelasteten Motorkomponenten”. In: (2010).
- [8] S. Antusch. *Investigations on the influence of soot in oil on engine wear: consideration of mechanochemical reactions*. XVII, 149. Berlin: Logos Verlag, 2008. ISBN: ISBN: 978-3-8325-2031-1 PPN: 287547043.
- [9] F. Zhao, M. Lai, and D. L. Harrington. “A Review of Mixture Preparation and Combustion Control Strategies for Spark-Ignited Direct-Injection Gasoline Engines”. In: *SAE Technical Paper* 412 (1997), SAE 970627. DOI: 10.4271/970627.
- [10] P. Whitaker et al. “Measures to Reduce Particulate Emissions from Gasoline DI engines”. In: *SAE International Journal of Engines* 4.1 (2011), pp. 1498–1512. ISSN: 19463936. DOI: 10.4271/2011-01-1219.
- [11] J. B. Heywood. *Internal Combustion Engine Fundamentals*. New York, NY, USA: McGraw Hill, 1988.
- [12] D. B. Kittelson. “Engines and nanoparticles: A review”. In: *Journal of Aerosol Science* 29.5-6 (1998), pp. 575–588. ISSN: 00218502. DOI: 10.1016/S0021-8502(97)10037-4.

- [13] F. Köppl et al. “Investigation of the Parameters Influencing the Spray-Wall Interaction in a GDI Engine - Prerequisite for the Prediction of Particulate Emissions by Numerical Simulation”. In: *SAE International Journal of Engines* 6.2 (2013), pp. 2013–01–1089. ISSN: 1946-3944. DOI: 10.4271/2013-01-1089. URL: <http://papers.sae.org/2013-01-1089/>.
- [14] S. Etikyala, L. Koopmans, and P. Dahlander. “Particulate emissions in a GDI with an upstream fuel source”. In: *SAE Technical Papers* 2019-April. April (2019). ISSN: 01487191. DOI: 10.4271/2019-01-1180.
- [15] J. Zhou et al. “Characteristics of near-nozzle spray development from a fouled GDI injector”. In: *Fuel* 219.92 (2018), pp. 17–29. ISSN: 00162361. DOI: 10.1016/j.fuel.2018.01.070. URL: <https://doi.org/10.1016/j.fuel.2018.01.070>.
- [16] H. Song et al. “The effects of deposits on spray behaviors of a gasoline direct injector”. In: *Fuel* (2016). ISSN: 00162361. DOI: 10.1016/j.fuel.2016.04.067.
- [17] A. Yamaguchi et al. “Spray Behaviors and Gasoline Direct Injection Engine Performance Using Ultrahigh Injection Pressures up to 1500 Bar”. In: *SAE International Journal of Engines* 15.1 (2021), pp. 167–183. ISSN: 19463944. DOI: 10.4271/03-15-01-0007.
- [18] A. N. Johansson, S. Hemdal, and P. Dahlander. “Experimental Investigation of Soot in a Spray-Guided Single Cylinder GDI Engine Operating in a Stratified Mode”. In: (2013). DOI: 10.4271/2013-24-0052. URL: <http://papers.sae.org/2013-24-0052/>.
- [19] Fangxi X. et al. “Effects of split and single injection strategies on particle number emission and combustion of a GDI engine”. In: *Proceedings of the Institution of Mechanical Engineers, Part D: Journal of Automobile Engineering* 233.5 (2019), pp. 1100–1114. DOI: 10.1177/0954407018759739. eprint: <https://doi.org/10.1177/0954407018759739>. URL: <https://doi.org/10.1177/0954407018759739>.
- [20] F. Leach et al. “Comparing the effect of different oxygenate components on PN emissions from GDI engines”. In: (2010).
- [21] F. Leach, R. Stone, and D. Richardson. “The influence of fuel properties on particulate number emissions from a direct injection spark ignition engine”. In: *SAE Technical Papers* 2 (2013). DOI: 10.4271/2013-01-1558.
- [22] S. Etikyala, L. Koopmans, and P. Dahlander. “Effect of Renewable Fuel Blends on PN and SPN Emissions in a GDI Engine”. In: *SAE Technical Papers*. 2020. SAE International, 2020. DOI: 10.4271/2020-01-2199.
- [23] J. M. E. Storey et al. “Exhaust Particle Characterization for Lean and Stoichiometric DI Vehicles Operating on Ethanol-Gasoline Blends”. In: *SAE Technical Papers*. 2012. DOI: 10.4271/2012-01-0437. URL: <https://www.sae.org/content/2012-01-0437/>.
- [24] M. Kaiadi et al. “Transient control of combustion phasing and Lambda in a 6-cylinder port-injected natural-gas engine”. In: *Proceedings of the Spring Technical Conference of the ASME Internal Combustion Engine Division* (2009), pp. 655–662. ISSN: 15296598. DOI: 10.1115/ICES2009-76004.
- [25] Z. Ivanov and V. Mihaylov. “Transient operation of a direct injection diesel engine”. In: *IOP Conference Series: Materials Science and Engineering* 614.1 (2019). ISSN: 1757899X. DOI: 10.1088/1757-899X/614/1/012008.

- [26] V. Berthome, D. Chalet, and J. F. Hetet. “Characterization of Particle Emissions of Turbocharged Direct Injection Gasoline Engine in Transients and Hot Start Conditions”. In: *Journal of Thermal Science* 30.6 (2021), pp. 2056–2070. ISSN: 1993033X. DOI: 10.1007/s11630-021-1420-9.
- [27] D. D. Brehob et al. “Stratified-charge engine fuel economy and emission characteristics”. In: *SAE Technical Papers* 724 (1998). ISSN: 26883627. DOI: 10.4271/982704.
- [28] F. Bonatesta, E. Chiappetta, and A. La Rocca. “Part-load particulate matter from a GDI engine and the connection with combustion characteristics”. In: *Applied Energy* (2014). ISSN: 03062619. DOI: 10.1016/j.apenergy.2014.03.030.
- [29] D. Brugge, J. L. Durant, and C. Rioux. “Near-highway pollutants in motor vehicle exhaust: A review of epidemiologic evidence of cardiac and pulmonary health risks”. In: *Environmental Health: A Global Access Science Source* 6 (2007), pp. 1–12. ISSN: 1476069X. DOI: 10.1186/1476-069X-6-23.
- [30] A. Seaton et al. “Particulate air pollution and acute health effects.” In: *Lancet* 345.8943 (1995), pp. 176–178. ISSN: 0140-6736. DOI: 10.1016/S0140-6736(95)90173-6.
- [31] M. Santibáñez-Andrade et al. “Air pollution and genomic instability: The role of particulate matter in lung carcinogenesis”. In: *Environmental Pollution* 229 (2017), pp. 412–422. ISSN: 18736424. DOI: 10.1016/j.envpol.2017.06.019.
- [32] D. Hu et al. “Associations of phthalates exposure with attention deficits hyperactivity disorder: A case-control study among Chinese children”. In: *Environmental Pollution* 229 (2017), pp. 375–385. ISSN: 18736424. DOI: 10.1016/j.envpol.2017.05.089. URL: <http://dx.doi.org/10.1016/j.envpol.2017.05.089>.
- [33] F. R. Cassee et al. “Exposure, health and ecological effects review of engineered nanoscale cerium and cerium oxide associated with its use as a fuel additive”. In: *Critical Reviews in Toxicology* 41.3 (2011), pp. 213–229. ISSN: 10408444. DOI: 10.3109/10408444.2010.529105.
- [34] P. Price et al. “Cold start particulate emissions from a second generation di gasoline engine”. In: *SAE Technical Papers* (2007). DOI: 10.4271/2007-01-1931.
- [35] Y. Sun, W. Dong, and X. Yu. “Effects of coolant temperature coupled with controlling strategies on particulate number emissions in GDI engine under idle stage”. In: *Fuel* 225.April (2018), pp. 1–9. ISSN: 00162361. DOI: 10.1016/j.fuel.2018.03.075. URL: <https://doi.org/10.1016/j.fuel.2018.03.075>.
- [36] K. Aikawa, T. Sakurai, and J. J. Jetter. “Development of a predictive model for gasoline vehicle particulate matter emissions”. In: *SAE Technical Papers* 3.2 (2010), pp. 610–622. ISSN: 26883627. DOI: 10.4271/2010-01-2115.
- [37] H. Fu et al. “Impacts of Cold-Start and Gasoline RON on Particulate Emission from Vehicles Powered by GDI and PFI Engines”. In: *SAE Technical Papers* 2014-October (2014). ISSN: 01487191. DOI: 10.4271/2014-01-2836.
- [38] A. S. Ramadhas et al. “Impact of Ambient Temperature Conditions on Cold Start Combustion, Gaseous and Particle Emissions from Gasoline Engines”. In: *SAE Technical Papers* 2017-October.October (2017). ISSN: 01487191. DOI: 10.4271/2017-01-2286.
- [39] M. Athanasios et al. “Assessment of different technical options in reducing particle emissions from gasoline direct injection vehicles”. In: *Journal of Aerosol Science* 63

- (2013), pp. 115–125. ISSN: 0021-8502. DOI: <https://doi.org/10.1016/j.jaerosci.2013.05.004>. URL: <https://www.sciencedirect.com/science/article/pii/S0021850213001328>.
- [40] M. Urs, M. Martin, and F. Anna-Maria. “Comprehensive particle characterization of modern gasoline and diesel passenger cars at low ambient temperatures”. In: *Atmospheric Environment* 39.1 (2005), pp. 107–117. ISSN: 1352-2310. DOI: <https://doi.org/10.1016/j.atmosenv.2004.09.029>. URL: <https://www.sciencedirect.com/science/article/pii/S1352231004008799>.
- [41] F. Akihiro et al. “Chemical composition and source of fine and nanoparticles from recent direct injection gasoline passenger cars: Effects of fuel and ambient temperature”. In: *Atmospheric Environment* 124 (2016), pp. 77–84. ISSN: 1352-2310. DOI: <https://doi.org/10.1016/j.atmosenv.2015.11.017>. URL: <https://www.sciencedirect.com/science/article/pii/S1352231015305252>.
- [42] M. Melaika and S. Etikyala. “Particulates from a CNG DI SI Engine during Warm-Up”. In: (2021), pp. 1–15. DOI: 10.4271/2021-01-0630. Abstract.
- [43] S. Etikyala and P. Dahlander. “Soot Sources in Warm-Up Conditions in a GDI Engine”. In: *SAE Technical Papers* 2021 (2021), pp. 1–10. ISSN: 01487191. DOI: 10.4271/2021-01-0622.
- [44] R. Suarez-Bertoa and C. Astorga. “Impact of cold temperature on Euro 6 passenger car emissions”. In: *Environmental Pollution* 234 (2018), pp. 318–329. ISSN: 18736424. DOI: 10.1016/j.envpol.2017.10.096. URL: <https://doi.org/10.1016/j.envpol.2017.10.096>.
- [45] Regulation No. 83. *Uniform provisions concerning the approval of vehicles with regard to the emission of pollutants according to engine fuel requirements*. “E/ECE/324/Rev.1/Add.82/Rev.4”.
- [46] F. Steimle et al. “Systematic analysis and particle emission reduction of homogeneous direct injection SI engines”. In: *SAE Technical Papers* 2 (2013). DOI: 10.4271/2013-01-0248.
- [47] D. B. Sonntag et al. “Contribution of lubricating oil to particulate matter emissions from light-duty gasoline vehicles in Kansas City”. In: *Environmental Science and Technology* 46.7 (2012), pp. 4191–4199. ISSN: 0013936X. DOI: 10.1021/es203747f.
- [48] H. Jung, D. B. Kittelson, and M. R. Zachariah. “The influence of engine lubricating oil on Diesel nanoparticle emissions and kinetics of oxidation”. In: *SAE Technical Papers* 724 (2003). DOI: 10.4271/2003-01-3179.
- [49] R. Amirante et al. “Effects of lubricant oil on particulate emissions from port-fuel and direct-injection spark-ignition engines”. In: *International Journal of Engine Research* 18.5-6 (2017), pp. 606–620. ISSN: 20413149. DOI: 10.1177/1468087417706602.
- [50] P. Eastwood. *Particulate emissions from Vehicles*. 2008. ISBN: 9780470724552. DOI: 10.1016/S0026-0576(00)83894-5. URL: <https://linkinghub.elsevier.com/retrieve/pii/S0026057600838945>.
- [51] L. Pirjola et al. “Effects of fresh lubricant oils on particle emissions emitted by a modern gasoline direct injection passenger car”. In: *Environmental Science and Technology* 49.6 (2015), pp. 3644–3652. ISSN: 15205851. DOI: 10.1021/es505109u.
- [52] L. A. Sgro et al. “Investigating the origin of nuclei particles in GDI engine exhausts”. In: *Combustion and Flame* 159.4 (2012), pp. 1687–1692. ISSN: 00102180. DOI: 10.



- 1016/j.combustflame.2011.12.013. URL: <http://dx.doi.org/10.1016/j.combustflame.2011.12.013>.
- [53] M. Mittal, H. Schock, and G. Zhu. “In-cylinder combustion visualization of a direct-injection spark-ignition engine with different operating conditions and fuels”. In: *SAE Technical Papers* 9 (2012). DOI: 10.4271/2012-01-1644.
- [54] K. Choi et al. “Evaluation of Time-Resolved Nano-Particle and THC Emissions of Wall-Guided GDI Engine”. In: (2011). DOI: 10.4271/2011-28-0022. URL: <http://papers.sae.org/2011-28-0022/>.
- [55] C. Farron et al. “Particulate Characteristics for Varying Engine Operation in a Gasoline Spark Ignited, Direct Injection Engine”. In: (2011). DOI: 10.4271/2011-01-1220. URL: <http://papers.sae.org/2011-01-1220/>.
- [56] D. Sabathil et al. “The influence of DISI engine operating parameters on particle number emissions”. In: *SAE Technical Papers* (2011). DOI: 10.4271/2011-01-0143.
- [57] Wang Y. et al. “The impact of fuel compositions on the particulate emissions of direct injection gasoline engine”. In: *Fuel* 166 (2016), pp. 543–552. ISSN: 0016-2361. DOI: <https://doi.org/10.1016/j.fuel.2015.11.019>. URL: <https://www.sciencedirect.com/science/article/pii/S0016236115011692>.
- [58] S. Florio et al. “Effect of Octane Number Obtained with Different Oxygenated Components on the Engine Performance and Emissions of a Small GDI Engine”. In: *SAE/JSAE 2014 Small Engine Technology Conference & Exhibition*. SAE International, 2014. DOI: <https://doi.org/10.4271/2014-32-0038>. URL: <https://doi.org/10.4271/2014-32-0038>.
- [59] L. Chen et al. “Characterizing particulate matter emissions from GDI and PFI vehicles under transient and cold start conditions”. In: *Fuel* 189 (2017), pp. 131–140. ISSN: 00162361. DOI: 10.1016/j.fuel.2016.10.055. URL: <http://dx.doi.org/10.1016/j.fuel.2016.10.055>.
- [60] A. J. Corning. “Review of Vehicle Engine Efficiency and Emissions”. In: (2020), pp. 1–29. DOI: 10.4271/2020-01-0352. Abstract.
- [61] M. Albrecht et al. “The Influence of Fuel Composition and Renewable Fuel Components on the Emissions of a GDI Engine”. In: *SAE Technical Paper Series* 1 (2020). DOI: 10.4271/2020-37-0025.
- [62] A. O. G. Abdalla and D. Liu. “Dimethyl carbonate as a promising oxygenated fuel for combustion: A review”. In: *Energies* 11.6 (2018), pp. 1–20. ISSN: 19961073. DOI: 10.3390/en11061552.
- [63] Y. Chen et al. “Emissions of automobiles fueled with alternative fuels based on engine technology: A review”. In: *Journal of Traffic and Transportation Engineering (English Edition)* 5.4 (2018), pp. 318–334. ISSN: 20957564. DOI: 10.1016/j.jtte.2018.05.001. URL: <https://doi.org/10.1016/j.jtte.2018.05.001>.
- [64] Y. Cao. “Operation and Cold Start Mechanisms of Internal”. In: *SAE Technical Paper* 2007-01-36.724 (2013), pp. 1–6.
- [65] M. M. Maricq, D. H. Podsiadlik, and R. E. Chase. “Examination of the size-resolved and transient nature of motor vehicle particle emissions”. In: *Environmental Science and Technology* 33.10 (1999), pp. 1618–1626. ISSN: 0013936X. DOI: 10.1021/es9808806.

- [66] M. M. Maricq et al. "Vehicle exhaust particle size distributions: A comparison of tailpipe and dilution tunnel measurements". In: *SAE Technical Papers* 724 (1999). ISSN: 26883627. DOI: 10.4271/1999-01-1461.
- [67] N. Y. Rojas. "Diesel Exhaust System Influences on Transient Particulate Emissions and Particle Size Distribution". In: *Department of Fuel and Energy Ph.D* (2001).
- [68] T. Yokoi. "Measurement repeatability improvement for particle number size distributions from diesel engines". In: *JSAE Review* 22.4 (2001), pp. 545–551. ISSN: 03894304. DOI: 10.1016/s0389-4304(01)00136-9.
- [69] H. Burtscher et al. "Separation of volatile and non-volatile aerosol fractions by thermodesorption : instrumental development and applications". In: 32 (2001), pp. 427–442.
- [70] J. Jang et al. "The Effect of Engine Oil on Particulate Matter , Emissions and Fuel Economy in Gasoline and Diesel Vehicle". In: *SAE International* (2015). DOI: 10.4271/2014-01-2837. Copyright.
- [71] H. Seong, K. Lee, and S. Choi. "Effects of engine operating parameters on morphology of particulates from a gasoline direct injection (GDI) engine". In: *SAE Technical Papers* 11 (2013). ISSN: 26883627. DOI: 10.4271/2013-01-2574.
- [72] A. Khosousi et al. "Experimental and numerical study of soot formation in laminar coflow diffusion flames of gasoline/ethanol blends". In: *Combustion and Flame* (2015). ISSN: 00102180. DOI: 10.1016/j.combustflame.2015.07.029.
- [73] M. Salamanca et al. "The effect of ethanol on the particle size distributions in ethylene premixed flames". In: *Experimental Thermal and Fluid Science* (2012). ISSN: 08941777. DOI: 10.1016/j.expthermflusci.2012.04.006.
- [74] G. Wallace et al. "Ethyl Tertiary Butyl Ether - A Review of the Technical Literature". In: *SAE International Journal of Fuels and Lubricants* 2.1 (2009), pp. 940–952. ISSN: 1946-3960. DOI: 10.4271/2009-01-1951.
- [75] Z. Zhang et al. "Combustion and particle number emissions of a direct injection spark ignition engine operating on ethanol/gasoline and n-butanol/gasoline blends with exhaust gas recirculation". In: *Fuel* (2014). ISSN: 00162361. DOI: 10.1016/j.fuel.2014.04.052.
- [76] S. Etikyala, L. Koopmans, and P. Dahlander. "History Effect on Particulate Emissions in a Gasoline Direct Injection Engine". In: *SAE International Journal of Engines* 15.3 (2021), pp. 1–11. ISSN: 19463944. DOI: 10.4271/03-15-03-0999.
- [77] S. Sakai, M. Hageman, and D. Rothamer. "Effect of equivalence ratio on the particulate emissions from a spark-ignited, direct-injected gasoline engine". In: *SAE Technical Papers* 2 (2013). ISSN: 26883627. DOI: 10.4271/2013-01-1560.
- [78] T. Alger et al. "The role of EGR in PM emissions from gasoline engines". In: *SAE Technical Papers* 3.1 (2010), pp. 85–98. ISSN: 26883627. DOI: 10.4271/2010-01-0353.
- [79] P. Dahlander et al. "Particulates in a GDI Engine and Their Relation to Wall-Film and Mixing Quality". In: (2022), pp. 1–11. DOI: 10.4271/2022-01-0430. Received.

# List of Figures

1.1	Sector split emissions of primary and secondary fine particulate emissions by particulate mass (PM10) [Source: EAA 18] . . . . .	5
1.2	Scope of research work in this thesis . . . . .	10
2.1	The NEDC drive cycle test sequence and the associated PN emissions from PFI and GDI engines with equal swept volumes. PN emissions are particularly high during cold starts, engine warm-up, transients, and high load drive phases [10]. . . . .	19
2.2	Illustration of a typical particulate found in engine exhaust [45] . . . . .	21
2.3	Image of a fuel spray injected into the cylinder of a GDI engine (SOI: -320 bTDC) . . . . .	22
2.4	Photographs of a GDI fuel injector before and after usage [15] . . . . .	23
2.5	Particle size distribution for a GDI engine at a load of 5 bar IMEP and an engine speed of 1500 rpm. The dashed line indicates the regulatory limit of 23 nm for PN emissions. . . . .	25
2.6	Influence of fuel injection timing (SOI) on particulate (PN) emissions at an engine load of 5 bar IMEP at 1500 rpm . . . . .	26
3.1	Schematic depiction of the dual injector setup showing the centrally mounted DI injector and a PFI injector mounted 500 mm upstream in a custom manifold. . . . .	32
3.2	Measurement matrix showing the central composite face experimental design. The test points are shown in blue. . . . .	34
3.3	Setup of optical access to combustion chamber showing assembly of (a) light source, (b) endoscope and (c) high-speed camera . . . . .	37
3.4	Schematic of experimental setup showing cRIO and engine controller along with sampling of raw exhaust along with endoscope view into the cylinder . . . . .	37
3.5	PN emissions from 10 repeats of pre-conditioning for a baseline load of 9 bar NMEP and SOI of -310 CAD at an engine speed of 2000 rpm . . . . .	39
3.6	Load transient sequences and load variation as functions of the cycle number and time at an engine speed of 2000 rpm. Cycles that were filmed are indicated by pictures of cameras and a grey background . . . . .	40
3.7	Evolution of the cylinder pressure, intake pressure, and resulting NMEP during a load transient at 2000 rpm with a coolant temperature of 15 °C. . . . .	41
3.8	Key components of the DMS500 particle size measurement system [Combustion 16] . . . . .	43

3.9	Measurement apparatus used to show switching enabled to sample engine exhaust with and without thermodenuder . . . . .	44
3.10	Working principle of a thermodenuder showing the removal of volatile organic compounds from engine out particles . . . . .	44
3.11	Frequency analysis to locate soot sources based on single shot combustion images captured at 50 CAD from ignition mid-way through three load transients (at 6bar NMEP). Coolant temperature = 15 °C, SOI = -310 CAD, engine speed = 2000 rpm. . . . .	45
5.1	PN in raw exhaust at 7 bar IMEP and 1500 rpm. PN emissions are highest when using DI exclusively and fall as the PFI contribution increases. [14]	54
5.2	Solid PN (#/cc) with diameters below 23 nm in exhaust samples passed through a thermodenuder for PFI contributions between 0 and 100%. Results obtained at an engine load of 7 bar IMEP and engine speeds between 1500 and 2500 rpm. [14] . . . . .	55
5.3	Effect of start of injection (SOI) and fuel blends on raw exhaust PN at lower load of 4.5 bar IMEP and 2000 rpm [22] . . . . .	57
5.4	Effect of start of injection (SOI) and fuel blends on raw exhaust PN at a higher load of 9 bar IMEP and 2000 rpm [22] . . . . .	58
5.5	PN concentrations recorded with indicated coolant and engine oil temperatures, -310 CAD injection timing and 200 bar injection pressure. 1000 rpm/ 4.5 bar. The error bars correspond to $\pm$ one standard deviation [43]	61
5.6	Relative frequencies of diffusion flames occurrence calculated from analyses of images of 20 combustion cycles at 50 CAD after ignition. Engine speed 1000 rpm, IMEP = 4.5 bar [43] . . . . .	62
5.7	PN emissions at 9 bar NMEP for 20,000 cycles and 2000 rpm with discrete step variation in SOI switching between -310 CAD and -340 CAD with 1000 cycles for each timing [76] . . . . .	64
5.8	PN emissions at 9 bar NMEP for 20,000 cycles and 2000 rpm with linear continuous variation in SOI changing from -180 CAD to -340 CAD and back to -180 CAD with accurately predefined timing for each cycle.[76] .	65
5.9	Single-shot images of the combustion chamber from one of the combustion cycles at 35 CAD during engine operation at an SOI of -250 CAD, -310 CAD, and -340 CAD, respectively, at 9 bar NMEP and 2000 rpm. Bottom row shows the relative frequency.[76] . . . . .	66
5.10	Post-transient PN measurements during stable operation at 12 bar NMEP at the end of the routine presented in Figure 3.6 for different experimental sets and coolant temperatures. . . . .	69
5.11	PN measurements over time at different engine coolant temperatures during the load transient routine shown in Figure 2. SOI = -310 CAD, engine speed = 2000 rpm, lambda = 1. . . . .	69

5.12	Single-shot images at 50 CAD from ignition during a load transient in which the load increases from 4 to 12 bar NMEP. The final column shows images after sustained operation at 12 bar NMEP. SOI = -310 CAD, engine speed = 2000 rpm, A/F =1. Each row shows an image captured during a single experimental replicate at the indicated coolant temperature. The incidence of diffusion flames clearly decreases with increasing temperature. Figure 5.11 shows the corresponding PN emissions. . . . .	70
5.13	Relative frequencies of yellow flames at different locations in the cylinder during the set 1 (baseline) transients at 50 CAD after ignition. SOI = -310 CAD, A/F =1, speed = 2000 rpm. Raw images are shown in Figure 5.12. . . . .	71
5.14	Relative frequencies of occurrence of diffusion flames calculated from analysis of images from multiples repeats of the load transient at 50 CAD after ignition using fuel E20. . . . .	73
5.15	Relative frequencies of occurrence of diffusion flames calculated from analysis of images from multiples repeats of the load transient at 50 CAD after ignition using fuel E85. . . . .	74

# List of Tables

1.1	EU emissions standards for particulate emissions from GDI-powered vehicles.	7
3.1	Engine Specifications . . . . .	31
3.2	Properties of the tested fuels* . . . . .	35
3.3	Experimental test matrix and corresponding engine parameters . . . . .	35
3.4	Operating conditions for load transient experiments . . . . .	42